Chapter 2

Atom-light interaction

2.1 Physical system

In a classic paper in 1954, R. H. Dicke calculated the rate at which radiation is emitted spontaneously by a collection of two-level atoms[42]. By considering the entire collection of N_A atoms as a single quantum system, he found that under certain conditions the atoms in the excited state can cooperatively decay into the ground state by emitting light into a single mode at a rate $1/\tau_c \propto N_A\Gamma_0$ much faster than their incoherent emission rate $\Gamma_0 = 1/\tau_0$. The emission intensity I_{coh} is thereby collectively enhanced with $I_{\text{coh}} \propto N_A\hbar\omega_0/\tau_c \propto N_A^2$, relative to the incoherent emission intensity $I_{\text{inc}} \propto N_A\hbar\omega_0/\tau_0 \propto N_A$. Indeed, the initial investigations of non-trivial dynamics for the collective spontaneous emissions began with the studies of 'superradiance' for atoms localized in a sub-wavelength region ($|r| < \lambda_0$)[42,44].

In a subsequent paper[154], Dicke predicted that radiation into a particular mode could be enhanced (superradiance) or suppressed (subradiance) for a spatially extended sample $|r| \gg \lambda_0$, depending upon the relative spatial phases of the atoms[44,155]. In this case, superradiance is manifested by a quantum analogue of Bragg reflection of light on an atomic phase grating. Unlike the case for sub-wavelength samples $|r| < \lambda_0$, where the initial spontaneous emission of an inverted atomic system leads to a phase coherence between the atomic dipoles due to the intrinsic indistinguishability in the emission process, the superradiant emission of an extended sample is also associated with the classical constructive interference of the wavelets produced by periodically located scattering sites in the "forward" direction set by the sample geometry. Such collective spontaneous emissions over extended samples have been observed in a wide variety of physical systems, including the observations of superradiance in molecular rotational and Rydberg transitions[156,157] as well as in optical transitions[158–160]. More recently, superradiant Rayleigh emission has been observed in light scattering experiments with Bose Einstein condensates[161].

In the quest to distribute quantum coherence and entanglement over quantum networks[1,162], there has been significant interest in the Raman interaction of light with atomic ensembles consisting of a large collection of identical atoms at the single-photon level[4,48] (chapters 3–10). In this chapter, I begin with an atom-light interaction Hamiltonian in Dicke's approximation leading to a classic type of collective spontaneous

fluorescence (for $|r| < \lambda_0$) and introduce basic notations used throughout this thesis (section 2.2). Then, I discuss the steady-state solutions for spontaneous Raman interaction which creates non-classical atom-photon correlations (section 2.3), and demonstrate that the parametric interaction can be used as quantum resources (section 2.4). I also describe the equation of motions for the collective matter-light interaction via the adiabatic passage of dark-state polaritons (section 2.5). Finally, I discuss two dominant decoherence mechanisms, which result in spin-wave dissipations and finite memory time (section 2.6).

2.2 Superradiance for a collection of two-level atoms

We consider an ensemble of N_A two-level atoms at positions $\vec{r}_i$ with $i \in \{1, \cdots, N_A\}$. The sample is comprised of ground and excited states ($|g\rangle, |e\rangle$), separated by an energy of $\hbar\omega_0$. Here, we introduce the raising and lowering single-atom operators in terms of Pauli spin operators $\hat{\sigma}_i^+$ ($\hat{\sigma}_i^-$) $= |e\rangle_i\langle g|$ ($|g\rangle_i\langle e|$), and the inversion operator as $\hat{\sigma}_{z,i} = \frac{1}{2}(|e\rangle_i\langle e| - |g\rangle_i\langle g|)$. The electric dipole operator is then given by $\hat{\mathcal{D}}_i = (\hat{\sigma}_i^+ + \hat{\sigma}_i^-)d_0\vec{\epsilon}_{\rm a}$, where d_0 is the matrix element for the transition $|g\rangle \leftrightarrow |e\rangle$ and $\vec{\epsilon}_{\rm a}$ is the polarization vector for the atomic transition. We introduce the positive and negative frequency components of the electric fields

$$\vec{E}^+(\vec{r}) = \sum_{\vec{k},\epsilon} \mathcal{E}_{\vec{k},\epsilon}\hat{a}_{\vec{k},\epsilon}e^{i\vec{k}\cdot\vec{r}}\vec{\epsilon}_\gamma \tag{2.1}$$

$$\vec{E}^-(\vec{r}) = \sum_{\vec{k},\epsilon} \mathcal{E}^*_{\vec{k},\epsilon}\hat{a}^\dagger_{\vec{k},\epsilon}e^{-i\vec{k}\cdot\vec{r}}\vec{\epsilon}^*_\gamma, \tag{2.2}$$

where $\mathcal{E}_{\vec{k},\epsilon}(\vec{r})$ is the slowly-varying amplitude and $\vec{\epsilon}_\gamma$ is the optical polarization vector, for which we assumed a plane-wave expansion with $\mathcal{E}_{\vec{k},\epsilon}(\vec{r}) = -i\sqrt{\frac{\hbar ck}{2\epsilon_0\mathcal{V}}}$.

We can then write the atom-light Hamiltonian for an ensemble of N_A two-level atoms as

$$\hat{H}_{\rm ensemble} = \sum_i^{N_A} \hbar\omega_0\hat{\sigma}_{z,i} + \sum_{\vec{k}} \hbar\omega_{\vec{k}}\hat{a}^\dagger_{\vec{k}}\hat{a}_{\vec{k}} - \sum_i^{N_A}\left(\vec{E}^+(\vec{r}) + \vec{E}^-(\vec{r})\right)\cdot\hat{\mathcal{D}}_i, \tag{2.3}$$

where $\{\hat{a}_{\vec{k}}, \hat{a}^\dagger_{\vec{k}}\}$ are the mode operators for wave-vector $\vec{k}$ [a].

2.2.1 Dicke Hamiltonian

Superradiance is a transient coherent process[b] involving a collective mode of all the N_A atoms in the sample. In the collective mode, correlation and order between the dipole moments arise through spontaneous emissions in an inverted system (initial state with $|\Psi(t=0)\rangle = |e\cdots e\rangle$), due to the intrinsic indistinguishability in the emission processes of the individual atoms. After a delay t_0, the initial spontaneously emitted photons build up the coherences among the atoms, leading to a superradiant pulse. From Eq. 2.3, we write the multi-mode theory of the Dicke Hamiltonian ($|r| < \lambda_0$) (in the electric dipole and rotating wave approximations) and treat the atomic states (labeled a) as a system and electromagnetic modes (labeled γ) as a Markovian bath. The Dicke Hamiltonian is given by

$$\hat{H}_{\rm Dicke} = \underbrace{\hbar\omega_0\hat{S}_z}_{\hat{H}_{\rm a}} + \underbrace{\sum_{\vec{k}} \hbar\omega_{\vec{k}}\hat{a}^\dagger_{\vec{k}}\hat{a}_{\vec{k}}}_{\hat{H}_\gamma} + \underbrace{\sum_{\vec{k}}\left(\hbar g_{\vec{k}}\hat{S}_0^+\hat{a}_{\vec{k}} + h.c.\right)}_{\hat{H}_{\rm a\gamma}}, \tag{2.4}$$

[a] We implicitly include the polarization ϵ by absorbing the notation $(\vec{k},\epsilon) \to \vec{k}$.

[b] Other notable examples of transient cooperative effects include optical free induction decay and photon echo.

where $h.c.$ is a hermitian conjugate of the term $\hbar g_{\vec{k}} \hat{S}_0^+ \hat{a}_{\vec{k}}$, $\hbar g_{\vec{k}} = i\sqrt{\frac{\hbar c k d_0^2}{2\epsilon_0 \mathcal{V}}} \vec{\epsilon}_\gamma \cdot \vec{\epsilon}_\mathrm{a}$ is the single-atom single-photon coupling constant, $\vec{\epsilon}_{\gamma,\mathrm{a}}$ are the polarization vectors of the photon and the atomic dipole, and $\mathcal{V}$ is the coherence volume. Here, we used collective lowering and raising operators

$$\hat{S}_{\vec{k}}^- = \sum_i e^{i\vec{k}\cdot\vec{r}_i} \hat{\sigma}_i^- \simeq \hat{S}_0^- = \sum_i \hat{\sigma}_i^- \tag{2.5}$$

$$\hat{S}_{\vec{k}}^+ = \sum_i e^{-i\vec{k}\cdot\vec{r}_i} \hat{\sigma}_i^+ \simeq \hat{S}_0^+ = \sum_i \hat{\sigma}_i^+, \tag{2.6}$$

and the collective inversion operator

$$\hat{S}_z \simeq \sum_i \hat{\sigma}_i^z. \tag{2.7}$$

In addition, we define the total angular momentum operator (also known as the length of the Bloch vector $\vec{\hat{S}}_k$) as

$$\hat{S}^2 = \frac{1}{2}(\hat{S}_0^+ \hat{S}_0^- + \hat{S}_0^- \hat{S}_0^+) + \hat{S}_z. \tag{2.8}$$

In writing Eqs. 2.4–2.6, we assumed the sub-wavelength condition $e^{i\vec{k}\cdot\vec{r}_i} \simeq e^{i\vec{k}\cdot\vec{r}_0}$ for $^\forall i$ ($\hat{S}_{\vec{k}} \simeq \sum_i \hat{\sigma}_i^-$), leading to the introduction of collective symmetric states $|S, m\rangle$ of $\hat{S}_z$ and $\hat{S}_{\vec{k}}$[c].

2.2.2 Collective spin states

Collective spin states $|S, m\rangle$ for the maximum angular momentum $S = N/2$ are given by (ref.[43])

$$|S, m\rangle = \sqrt{\frac{(S+m)!}{N!(S-m)!}} (\hat{S}_0^-)^{S-m} |e \cdots e\rangle, \tag{2.9}$$

with $-S \leq m \leq S$. The collective state $|N_A/2, m\rangle$ in Eq. 2.9 represents a fully symmetric state whereby $(N_A/2 + m)$ atoms are in the excited state $|e\rangle$ and $(N_A/2 - m)$ atoms are in the ground state $|g\rangle$. The collective spin states $|S, m\rangle$ are simultaneous eigenstates of Eqs. 2.7–2.8 with the following relations

$$\hat{S}_z |S, m\rangle = m|S, m\rangle \tag{2.10}$$

$$\hat{S}^2 |S, m\rangle = S(S+1)|S, m\rangle. \tag{2.11}$$

Similarly, the collective raising and lowering operators $\hat{S}_0^\pm$ acting on $|S, m\rangle$ are

$$\hat{S}_0^\pm |S, m\rangle = \sqrt{(S \mp m)(S \pm m + 1)} |S, m \pm 1\rangle. \tag{2.12}$$

[c]For $|r| < \lambda_0$ in the optical regime, one cannot neglect the effect of van der Waals force $\sim 1/r_{ij}^3$. I refer to ref.[44] for further discussions of non-ideal superradiance in the presence of dipole-dipole coupling between the atoms.

The collective spin operators follow the commutator relations

$$\left[\hat{S}_0^+, \hat{S}_0^-\right] = 2\hat{S}_z \tag{2.13}$$

$$\left[\hat{S}_z, \hat{S}_0^\pm\right] = \pm\hat{S}_0^\pm. \tag{2.14}$$

We will use the language of collective spin algebra in the context of quantum many-body theory in chapter 9 to study the thermal behavior of entanglement in quantum spin models.

Since the Dicke Hamiltonian $\hat{H}_{\text{Dicke}}$ in Eq. 2.4 commutes with the operator $\hat{S}^2$, $\langle\hat{S}^2\rangle$ is a constant of motion. On the other hand, $[\hat{S}_z, \hat{H}_{\text{Dicke}}] \neq 0$. Thus, as we will discuss in the next section, we can expect that the inverted atomic system ($|\Psi(t=0)\rangle = |e\cdots e\rangle$) undergoes a series of cascade emissions with the atomic state confined in a ladder formed by $(2S+1)$ equidistant energy levels $E_m = m\hbar\omega_0$ of the symmetric collective states $|S, m\rangle$ shown in Fig. 2.1a, analogous to the case of spontaneous emission of a spin with angular momentum S.

2.2.3 Superradiant emission for an atomic ensemble in a sub-wavelength volume

Since the system-reservoir Hamiltonian is $\hat{H}_{\text{a}\gamma} = \sum_{\vec{k}}(\hbar g_{\vec{k}}\hat{S}_0^+\hat{a}_{\vec{k}}e^{i(\omega_0-\omega_k)t} + h.c.)$ in the interaction picture (Eq. 2.4), we can write the real part[d] of the master equation (in the Born-Markov approximation[e]) with $\frac{d}{dt}\hat{\rho}_{\text{a}}(t)|_{\text{real}} = -\frac{1}{\hbar^2}\text{Tr}_\gamma\left(\int_0^t dt'[\hat{H}_{\text{a}\gamma}(t), [\hat{H}_{\text{a}\gamma}(t'), \hat{\rho}_{\text{a}}(t)\otimes\hat{\rho}_\gamma(0)]]\right)$ following the standard procedures [164–166] as

$$\begin{aligned}\frac{d}{dt}\hat{\rho}_{\text{a}}(t)|_{\text{real}} &= -\frac{\Gamma_0}{2}\overline{n}_\gamma(\hat{S}_0^-\hat{S}_0^+\hat{\rho}_{\text{a}} - 2\hat{S}_0^+\hat{\rho}_{\text{a}}\hat{S}_0^- + \hat{\rho}_{\text{a}}\hat{S}_0^-\hat{S}_0^+) \\ &\quad -\frac{\Gamma_0}{2}(\overline{n}_\gamma+1)(\hat{S}_0^+\hat{S}_0^-\hat{\rho}_{\text{a}} - 2\hat{S}_0^-\hat{\rho}_{\text{a}}\hat{S}_0^+ + \hat{\rho}_{\text{a}}\hat{S}_0^+\hat{S}_0^-),\end{aligned} \tag{2.16}$$

where $\Gamma_0 = k^3 d_0^2/(3\pi\epsilon_0\hbar)$ is the single-atom spontaneous emission rate in the Wigner-Weisskopf theory of spontaneous decay.

To describe superradiance in the optical domain, we may approximate the reservoir modes γ as vacuum states with zero mean thermal occupation ($\overline{n}_\gamma = 0$). Then, the surviving term in this master equation (2nd term) describes a symmetric collective damping process for the system, cascading from the initial totally

[d] Note that the dispersive imaginary part of the master equation gives rise to collective Lamb shift and van der Waals interaction [44]. Namely, we find

$$\frac{d}{dt}\hat{\rho}_{\text{a}}(t)|_{\text{imaginary}} = -\frac{id_0^2}{4\pi\epsilon_0}\left[\sum_{i>j}\frac{1}{r_{ij}^3}\left[1-\frac{3(\vec{\epsilon}_{\text{a}}\cdot\vec{r}_{ij})^2}{r_{ij}^2}\right]\hat{\sigma}_i^+\hat{\sigma}_j^+, \hat{\rho}_{\text{a}}\right]. \tag{2.15}$$

The superradiance for Eq. 2.16 occurs because of the indistinguishability in the emission pathways among the atoms. The dispersive van der Waals interaction (Eq. 2.15) has a characteristic dipole-dipole coupling $g_{vdW} \simeq \frac{|d_0|^2}{4\pi\epsilon_0 r_{ij}^3}$, where the relative strength to Γ_0 is $\frac{g_{vdW}}{\Gamma_0} \simeq \frac{1}{10\pi}\left(\frac{\lambda_0}{r_{ij}}\right)^3$. For $|r| \ll \lambda_0$, the frequency shifts of this dipole-dipole interaction may break the symmetric behavior of superradiance as discussed here. The full analysis including van der Waals dephasing is out of scope for the current discussion, and I refer to refs. [44,163] for a detailed analysis.

[e] For sufficiently large N_A, the Markovian approximation $\hat{\rho}_\gamma(t') \simeq \hat{\rho}_\gamma(0) = \prod_{\vec{k}}|0\rangle_{\vec{k}}\langle 0|$ may break down, leading to oscillatory superradiant emissions [164,165].

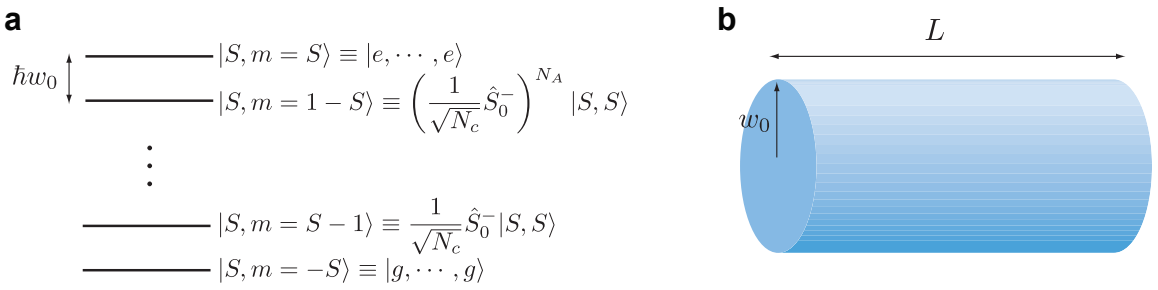

Figure 2.1: **Superradiant states and atomic Fresnel number.** **a**, Energy levels for the collective spin states. A ladder of symmetric collective spin states of maximal angular momentum $S = N_A/2$ is shown for $m \in \{-S, -S+1, \cdots, S-1, S\}$. N_c is the normalization constant. **b**, Pencil-shaped atomic ensemble. The geometric angle is given by $\theta_g = \sqrt{\pi w_0^2/L}$, whereas the diffraction angle is $\theta_d = \lambda_0/\sqrt{\pi w_0^2}$.

inverted state $|\Psi(t = 0)\rangle = |S, S\rangle$ ($|e \cdots e\rangle$) to lower symmetric collective states $|S, m\rangle$ (progressively decaying from $m = N_A/2$ to $m = -N_A/2$) in the subspace of $S = N_A/2$ (Fig. 2.1a).

Indeed, in the quantum jump picture, we can write the short-time (δt) evolution of the atomic state $\hat{\rho}_{\rm a}(t)$ as (Eq. 2.16)

$$\hat{\rho}_{\rm a}(t+\delta t) \simeq \underbrace{\left(1 - \frac{\Gamma_0 \delta t}{2}\hat{S}_0^+\hat{S}_0^-\right)\hat{\rho}_{\rm a}(t)\left(1 - \frac{\Gamma_0 \delta t}{2}\hat{S}_0^+\hat{S}_0^-\right)}_{\text{“no” photon loss}} + \underbrace{\Gamma_0 \delta t \hat{S}_0^- \hat{\rho}_{\rm a}(t)\hat{S}_0^+}_{\text{“yes” photon loss}} + \mathcal{O}(\delta t^2), \tag{2.17}$$

with the two terms corresponding to the conditional density matrices for zero and single spontaneous emitted photons, respectively. Since the collective jump operators $\hat{S}_0^{\pm}$ cannot alter the symmetry (and the total angular momentum S) of $\hat{\rho}_{\rm a}(t)$, the time-evolution of $\hat{\rho}_{\rm a}(t)$ from the initially symmetric state $|\Psi(t = 0)\rangle$ with total inversion will remain in the $S = N_A/2$ manifold with a transition probability from $|S, m\rangle$ to $|S, m-1\rangle$ given by $p(|S, m\rangle \to |S, m-1\rangle) = \Gamma_0 \delta t \langle \hat{S}_0^+ \hat{S}_0^- \rangle = \Gamma_0 \delta t (S + m)(S - m + 1)$. In particular, for $m = 0$, we find a collectively enhanced emission of $p(|S, 0\rangle \to |S, -1\rangle) \simeq \frac{\Gamma_0 \delta t N_A^2}{4}$, relative to the transition probability $\Gamma_0 \delta t N_A$ for a collection of independent atoms ($\Gamma_0 \delta t$ for single atoms).

The equation of motion for the collective spin operators $\{\hat{S}_0^{\pm}(t), \hat{S}_z(t)\}$ can be solved analytically from the master equation (Eq. 2.16) in the semi-classical approximation. Using the commutator relationships (Eqs. 2.13–2.14), we obtain the following differential equations (Eq. 2.16)

$$\frac{d}{dt}\langle \hat{S}_0^- \rangle = -\Gamma_0 \langle \hat{S}_z \hat{S}_0^+ \rangle \tag{2.18}$$

$$\frac{d}{dt}\langle \hat{S}_z \rangle = -\Gamma_0 \langle \hat{S}_0^+ \hat{S}_0^- \rangle. \tag{2.19}$$

In the semi-classical approximation (i.e., taking operators as c-numbers), we solve the equations of motions (Eqs. 2.18–2.19) and obtain $\langle \hat{S}_z(t) \rangle \simeq -S \tanh(\Gamma_0 S(t - t_d))$. This leads to a superradiant emission intensity of $I_c = -\Gamma_0 \frac{d\langle \hat{S}_z \rangle}{dt} = \frac{N_A^2 \Gamma_0}{4} \text{sech}^2\left(\frac{N_A \Gamma_0}{2}(t - t_d)\right)$.

2.2.4 Superradiance for extended atomic ensembles

The dynamics of multimode superradiance for extended samples[167,168] is more complex than the classic example of Dicke superradiance[42] in section 2.2.3, as the master equation involves various spatial phases $\vec{k}\cdot\vec{r}_i$ (thus, the geometry of the atomic sample) as well as a second-order propagation equation (i.e., Maxwell-Bloch equation, see also Eq. 2.39) through the atomic sample of length $L \gg \lambda_0$ (see Fig. 2.1b). For the current discussion, it suffices to say that if the Fresnel number $F_{\mathrm{a}} = \pi w_0^2/L\lambda_0$ is $\simeq 1$ for the atomic sample[f] ($F \simeq 1$ for our experimental parameters, see section 2.3.2.2), the propagation equations of the field for the 'pencil shaped' sample can be well approximated to a one-dimensional model[44,70,167,168]. The superradiant emission takes place along the elongated direction $\vec{k}'$ of the sample (so-called "end-fire mode")[161], for which the collective variables $\vec{S}_{\vec{k}} = \sum_i e^{i\vec{k}\cdot\vec{r}_i}\vec{\sigma}_i$ are "phase-matched." In this case, the so-called 'shape function' $f(\vec{k},\vec{k}') = \frac{1}{N_A^2}\sum_{i,j}^{N_A}\exp[i(\vec{k}-\vec{k}')(\vec{r}_j-\vec{r}_i)]$ determines the phase-matching condition from the sample geometry[167], which results from the classical interferences of the emitted photons $\vec{k}'$ from the collection of atoms excited by a pump laser with a wave-vector $\vec{k}$.

[f] As shown in Fig. 2.1b, we can express the Fresnel number $F_{\mathrm{a}} = \theta_g/\theta_d$ as the ratio between the geometric and diffraction angles ($\theta_{g,d}$) with θ_g (θ_d) $= \sqrt{\pi w_0^2}/L$ ($\lambda_0/\sqrt{\pi w_0^2}$). For $F \gg 1$, several transverse modes are necessary to describe the field propagation through the atomic ensemble, whereas $F_{\mathrm{a}} \ll 1$ gives large diffraction angle. In our experiment, L is set, by design, approximately to the Rayleigh length z_R for the Hermite-Gaussian mode of our imaging system ($L \simeq z_R$), as our atomic sample is much larger than both $\{w_0, z_R\}$. Thus $F_{\mathrm{a}} = \pi w_0^2/L\lambda_0 = z_R/L \simeq 1$. This justifies the use of the Maxwell-Bloch equation with paraxial approximation in our analysis for sections 2.3–2.5.

2.3 Parametric atom-light interaction

The weak nonlinearity of spontaneous Raman scattering can generate strong non-classical correlations between the atoms and the scattered photons[169]. As we will discuss later in section 2.4, combined with the 'strong' nonlinear response of the system by a quantum measurement, an initially independent pairs of atomic ensembles can be prepared into a heralded entangled state by a nonlocal measurement (refs.[4,27,34], see chapter 3). A critical element is the initial atom-photon correlation generated from parametric atom-light interactions $\hat{H}_{\text{int}}^{(\text{par})} \sim \chi_p \hat{a}_\gamma \hat{S}_a + h.c.$. Such quantum resources form the basis of many experiments in this thesis (chapters 3–5).

The creation of atom-photon correlations can be qualitatively understood as follows (Fig. 2.2). As shown in Fig. 2.2a, we initially prepare all the atoms in their ground state $|\overline{g}\rangle = |g, \cdots, g\rangle$. Subsequently, an off-resonant 'write' laser (red-detuned from $|g\rangle \to |e\rangle$ transition with detuning Δ_w) induces a spontaneously Raman scattered photon ($|e\rangle \to |s\rangle$), called field 1 (denoted by γ_1), in the forward direction (with probability $\xi \ll 1$), whose photon-number state $|n\rangle_{\gamma_1}$ is correlated with the number states $|n\rangle_{\text{a}}$ of the atoms being transferred from the initial state $|g\rangle$ to a metastable ground state $|s\rangle$. As it is impossible (even in principle) to discern which atom $i \in \{1 \cdots N_A\}$ has been transferred to $|s_i\rangle$ (i.e., the *which-atom* information), the number state of the atoms is associated with a collective atomic mode $\vec{\hat{S}}_{gs} = \frac{1}{N_A} \sum_i^{N_A} e^{i(\vec{k}_w - \vec{k}_1)\cdot \vec{r}_i} \vec{\hat{\sigma}}_{gs}$, corresponding to a 'spin wave' of a collective excitation. These spin-wave excitations are analogous to the symmetric superradiant states (but for *radiatively inactive* hyperfine ground state coherences $|g\rangle - |s\rangle$) in section 2.2.2. Thus, the classical writing laser drives the initial atom-field state to a two-mode squeezed state $|\Psi\rangle_{\text{a}\gamma_1} = \hat{U}_{\text{int}}^{(\text{par})} |\overline{g}\rangle = \sum_{n=0}^{\infty} c_n |n_{\text{a}}, n_{\gamma_1}\rangle$ with thermal distribution $|c_n|^2 = \frac{\overline{n}^n}{(\overline{n}+1)^{n+1}}$ through a coherent evolution of $\hat{U}_{\text{int}}^{(\text{par})} = e^{-i \int dt \hat{H}_{\text{int}}^{(\text{par})}(t)/\hbar}$, which display non-classical correlations between the two modes[72,73] (i.e., between the field 1 and the collective atomic mode). Any subsequent measurement on $|n\rangle_{\gamma_1}$ projects the spin sibling to a definite number state $|n\rangle_{\gamma_1}$ of collective excitations (section 2.4).

In this section, we describe a quantum theory for spontaneous Raman scattering in the regime of weak excitations $\xi \ll 1$ with an effective one-dimensional model. We decompose the atom-light interaction Hamiltonian for a Λ-level system by adiabatically eliminating the excited state. We also obtain the steady-state solutions for the atom-field system, which correspond to a model of non-degenerate parametric amplifier.

2.3.1 Spontaneous Raman interaction: Creating spin waves

Here, we consider an atomic ensemble consisting of N_A atoms in a Λ-level system. We assume a cylindrical atomic sample with radius w_0 and length L (Fig. 2.1b). As shown by Fig. 2.2a, the atomic ensemble interacts with a classical 'write' laser with Rabi frequency $\Omega_w(\vec{r}, t) e^{i\vec{k}_w \cdot \vec{r}}$ (where $\Omega_w(\vec{r}, t) = \tilde{\Omega}_w(t) u_w(\vec{r})$) and polarization $\vec{\epsilon}_w$, and a quantum field $\vec{\hat{E}}_1(\vec{r}, t)$, which we call field 1. Here, $u_w(\vec{r})$ is the mode function for a Hermite-Gaussian mode of the writing laser, and the positive frequency component of the quantum field

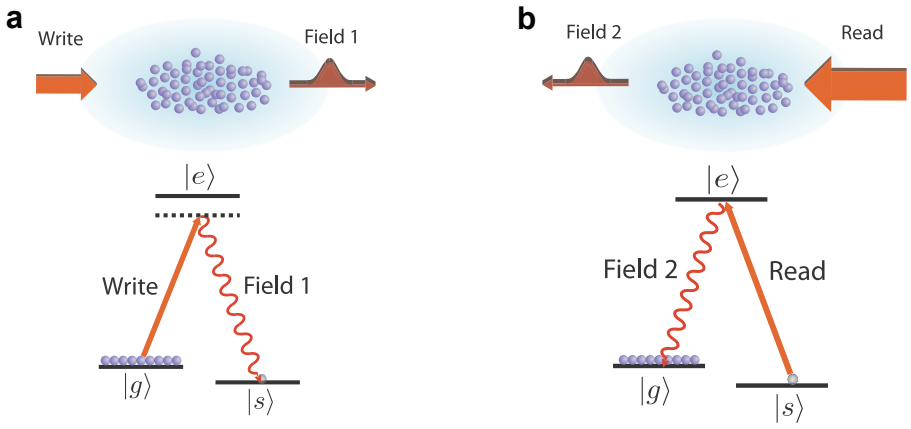

Figure 2.2: **Generating and retrieving collective excitations to photons. a**, Generating and storing single collective excitations. A weak write pulse illuminates the cold atomic sample, generating a Raman scattered photon, called field 1. The detection of a single photon in field 1 heralds the generation of a correlated single collective excitation $|\bar{s}\rangle$ in the ensemble. **b**, Retrieving single collective excitations to single photons. After a storage time τ, a strong read pulse maps the collective excitation to a single photon in field 2 via superradiant emission.

is expressed in terms of the normalized slowly-varying operator $\hat{\mathcal{E}}_1(\vec{r},t)$ with

$$\hat{\vec{E}}_1^+(\vec{r},t) = i\sqrt{\frac{\hbar w_1}{2\epsilon_0 \mathcal{V}_1}}\hat{\mathcal{E}}_1(\vec{r},t)e^{i\vec{k}_1\cdot\vec{r}}\vec{\epsilon}_1. \tag{2.20}$$

The slowly-varying operator $\hat{\mathcal{E}}_1(\vec{r},t)$ obeys the commutation relations

$$[\hat{\mathcal{E}}_1(\vec{r},t), \hat{\mathcal{E}}_1^\dagger(\vec{r}',t')] = \mathcal{V}_1\delta(\vec{r}_\perp - \vec{r}'_\perp)\delta(z - z' - c(t-t')) \tag{2.21}$$

where $\vec{r}_\perp = (x,y)$ is the transverse position vector and $\mathcal{V}_1$ is the field quantization volume.

As we described in the previous section, the writing laser is red-detuned by $\Delta_w = w_w - w_{ge}$ from the $|g\rangle \to |e\rangle$ transition, and we also include the two-photon detuning $\delta_{w1} = w_w - w_1 + w_{gs}$ for the 'field 1', where w_i with $i \in \{w,1\}$ are the respective angular frequencies for the writing laser and field 1, and w_{gs} is the hyperfine splitting for the ground states $|g\rangle - |s\rangle$. Both fields propagate approximately in the forward direction $\vec{k}_w(\vec{k}_1) \parallel \hat{z}$, and we treat the propagation of the weak quantized field in the paraxial approximation. In practice, we employ an off-axial excitation scheme pioneered by Balić *et al.*[75], with a small relative angle $\theta \leq 3^\circ$ between $\vec{k}_w$ and $\vec{k}_1$, such that $\vec{\epsilon}_1, \vec{\epsilon}_w \simeq \vec{\epsilon}_q$, where $\vec{\epsilon}_q$ is the polarization vector in the spherical basis[g].

[g] We decompose the polarization vector in the spherical tensor form,

$$\begin{aligned}\vec{\epsilon}_+ &= -\frac{1}{\sqrt{2}}(\hat{x} + i\hat{y}) \\ \vec{\epsilon}_- &= \frac{1}{\sqrt{2}}(\hat{x} - i\hat{y}) \\ \vec{\epsilon}_0 &= \hat{z}.\end{aligned}$$

2.3.1.1 Interaction Hamiltonian

In the weak depletion limit[h], where the Rabi frequency $\Omega_w(\vec{r},t)$ is constant over z, we can write the interaction Hamiltonian in the rotating wave approximation,

$$\begin{aligned}\hat{H}_s^{(\text{par})} &= \int d\vec{r} n_A(\vec{r})\{\hbar\Delta_w\hat{\sigma}_{ee}(\vec{r},t) - \hbar\delta_{w1}\hat{\sigma}_{ss}(\vec{r},t) \\ &\quad - \left[\hbar g_p\hat{\mathcal{E}}_1(\vec{r},t)e^{i\vec{k}_1\cdot\vec{r}}\hat{\sigma}_{es}(\vec{r},t) + \hbar\Omega_w(\vec{r},t)e^{i\vec{k}_w\cdot\vec{r}}\hat{\sigma}_{eg}(\vec{r},t) + h.c.\right]\},\end{aligned} \tag{2.22}$$

where $n_A(\vec{r})$ is the atomic density, $g_p = d_{es}\sqrt{\frac{w_{es}}{2\hbar\epsilon_0\mathcal{V}_1}}$ is the atom-photon coupling constant with dipole matrix element $d_{es} = \langle e|\hat{d}|s\rangle$. We take the quantization volume $\mathcal{V}_1$ as the sample volume. In writing the Hamiltonian $\hat{H}_s^{(\text{par})}$ in Eq. 2.22, we denoted the collective atomic variables defined *locally* at $\vec{r}$ (evaluated over a small volume[i] containing $N_{\vec{r}} \gg 1$ atoms) in the continuum limit ($\sum \to \int d\vec{r} n_A(\vec{r})$) of

$$\hat{\sigma}_{\mu\nu}(\vec{r},t) = \frac{1}{N_{\vec{r}}}\sum_i^{N_{\vec{r}}}\hat{\sigma}_{\mu\nu}^{(i)}e^{-iw_{\mu\nu}t}, \tag{2.23}$$

with single-atom operator $\hat{\sigma}_{\mu\nu}^{(i)} = |\mu\rangle_i\langle\nu|$. The collective variables follow the commutation relations,

$$[\hat{\sigma}_{\alpha\beta}(\vec{r},t),\hat{\sigma}_{\mu\nu}(\vec{r}',t)] = \frac{\mathcal{V}_1}{N_{\vec{r}}}\delta(\vec{r}-\vec{r}')(\delta_{\beta\mu}\hat{\sigma}_{\alpha\nu}(\vec{r},t) - \delta_{\nu\alpha}\hat{\sigma}_{\mu\beta}(\vec{r},t)). \tag{2.24}$$

In particular, the hyperfine ground-state coherence $\{\hat{\sigma}_{gs},\hat{\sigma}_{sg}\}$ follows the Bosonic commutator relations

$$[\hat{\sigma}_{sg}(\vec{r},t),\hat{\sigma}_{sg}^\dagger(\vec{r}',t)] \simeq \frac{\mathcal{V}_1}{N_{\vec{r}}}\delta(\vec{r}-\vec{r}')\hat{\sigma}_{gg}(\vec{r},t) + \mathcal{O}\left(\frac{1}{N_{\vec{r}}^2}\right) \tag{2.25}$$

in the weak excitation limit $\sigma_{gg} \simeq 1 \gg \sigma_{ee},\sigma_{ss}$.

2.3.1.2 Heisenberg-Lanvegin equations

In addition, the system $\hat{H}_s^{(\text{par})}$ interacts with a thermal reservoir (Markovian bath)

$$\hat{H}_r = \sum_{\vec{k},j}\hbar w_j\hat{r}_{\vec{k},j}^\dagger\hat{r}_{\vec{k},j} \tag{2.26}$$

at temperature T (mean photon number $\overline{n}_{\mu\nu}^{\text{th}}$) with reservoir mode operators $\{\hat{r}_{\vec{k},l}^\dagger,\hat{r}_{\vec{k},l}\}$ and with interaction Hamiltonian of the form

$$\hat{H}_{sr}^{(\mu\nu)} = \hbar\sum_{\vec{k},j}\left(g_{sr}(\vec{k},w_j)\hat{r}_{\vec{k},j}^\dagger\hat{\sigma}_{\mu\nu} + h.c.\right). \tag{2.27}$$

[h]This approximation is, strictly speaking, not valid for our laboratory parameters with optical depth $\tilde{d}_0(\Delta_w=0) > 10$ and small detuning $\Delta/\Gamma \simeq 2$ (chapters 3–9). In our experiments, the writing laser experience non-negligible amount of depletion as it propagates through the sample with $\Omega_w(\vec{r},t) \sim e^{-\tilde{d}_0(\Delta_w)z/L}$, where $\tilde{d}_0(\Delta_w)$ is the effective optical depth for the detuning Δ_w.

[i]The linear dimension $|\delta\vec{r}|$ of this volume must be large enough to contain macroscopic numbers of atoms, but small compared to the characteristic variation in the spin-wave amplitude: i.e., $|\delta\vec{r}| \ll \lambda_{gs} = \frac{2\pi}{|\vec{k}_w-\vec{k}_1|}$.

The total Hamiltonian including the respective reservoir modes for the atomic coherences $\sigma_{\mu\nu}$ is

$$\hat{H}_{\text{tot}} = \hat{H}_s^{(\text{par})} + \hat{H}_r + \sum_{\mu,\nu} \hat{H}_{sr}^{(\mu\nu)}. \tag{2.28}$$

In the Heisenberg-Langevin approach[143,164–166], we can describe the dynamics of the atomic operators (from Eq. 2.28) by a set of *self-consistent* equations of motions (ref.[143])

$$\partial_t \hat{\sigma}_{\mu\nu} = -\gamma_{\mu\nu}\hat{\sigma}_{\mu\nu} - \frac{i}{\hbar}[\hat{\sigma}_{\mu\nu}, \hat{H}_s^{(\text{par})}] + \hat{F}_{\mu\nu}. \tag{2.29}$$

The Langevin noise operators $\hat{F}_{\mu\nu}(\vec{r},t)$ arise from the system-reservoir interactions $\hat{H}_{sr}^{(\mu\nu)}$, and are associated with the decay term $(-\gamma_{\mu\nu}\hat{\sigma}_{\mu\nu})$ in Eq. 2.29, representing the dissipation of the atomic coherences $\hat{\sigma}_{\mu\nu}$ into the fluctuating reservoir modes (and vice versa). The exact form of $\hat{F}_{\mu\nu}(\vec{r},t)$ is not important, as they are δ-correlated ($\langle \hat{F}_{\mu\nu}^{\dagger}(t)\hat{F}_{\mu\nu}(t')\rangle_r = 2\gamma_{\mu\nu}\overline{n}_{\mu\nu}^{\text{th}}\mathcal{V}_1\delta(t-t')$ and $[\hat{F}_{\mu\nu}(t), \hat{F}_{\mu\nu}^{\dagger}(t')] = 2\gamma_{\mu\nu}\mathcal{V}_1\delta(t-t')$) and have zero reservoir average ($\langle \hat{F}_{\mu\nu}\rangle_r = 0$). In addition, the system-reservoir correlation function is given by $\langle \hat{\sigma}_{\mu\nu}^{\dagger}(t)\hat{F}_{\mu\nu}(t')\rangle = \gamma_{\mu\nu}\overline{n}_{\mu\nu}^{\text{th}}\mathcal{V}_1\delta(t-t')$. In the following discussion, we will assume vacuum states $\overline{n}_{\mu\nu}^{\text{th}} = 0$ for the reservoir modes[j].

Explicitly, the equations of motions for the optical coherences $\{\hat{\sigma}_{se}, \hat{\sigma}_{eg}\}$, and the ground-state coherence $\hat{\sigma}_{gs}$ are given by the following set of equations (with $\hat{\sigma}_{gg} \gg \hat{\sigma}_{ss}, \hat{\sigma}_{ee}$)

$$\partial_t\hat{\sigma}_{se} = -(\gamma_{se} + i(\Delta_w - w_{gs}) - i\delta_{w1})\hat{\sigma}_{se} + i\Omega_w e^{i\vec{k}_w\cdot\vec{r}}\hat{\sigma}_{sg} + \hat{F}_{se} \tag{2.30}$$

$$\partial_t\hat{\sigma}_{gs} = -(\gamma_{gs} - i\delta_{w1})\hat{\sigma}_{gs} - i\Omega_w e^{i\vec{k}_w\cdot\vec{r}}\hat{\sigma}_{es} + ig_p^*\hat{\mathcal{E}}_1 e^{-i\vec{k}_1\cdot\vec{r}}\hat{\sigma}_{ge} + \hat{F}_{gs} \tag{2.31}$$

$$\partial_t\hat{\sigma}_{eg} = -(\gamma_{eg} - i\Delta_w)\hat{\sigma}_{eg} - i\Omega_w^* e^{-i\vec{k}_w\cdot\vec{r}}\hat{\sigma}_{gg} + \hat{F}_{eg}. \tag{2.32}$$

2.3.1.3 Adiabatic elimination of excited state

In the following, we solve the steady-state solution for Heisenberg-Langevin equation of motion (Eqs. 2.30–2.32). If we assume the far off-resonant limit $\Delta_w \gg \gamma_{se}, \gamma_{eg}$ and the narrow-bandwidth $\delta w_w \ll \Delta_w$ of the write laser, we can adiabatically eliminate the excited state $|e\rangle$ and obtain the steady-state solutions for the optical coherences (i.e., $\partial_t\hat{\sigma}_{se} = \partial_t\hat{\sigma}_{eg} = 0$). Namely,

$$\hat{\sigma}_{se} \simeq -\frac{\Omega_w}{\Delta_w - w_{gs}}\left(1 + \frac{\delta_{w1} + i\gamma_{se}}{\Delta_w - w_{gs}}\right)e^{i\vec{k}_w\cdot\vec{r}}\hat{\sigma}_{sg} \tag{2.33}$$

$$\hat{\sigma}_{eg} \simeq -\frac{\Omega_w^*}{\Delta_w}\left(1 - i\left(\frac{\gamma_{eg}}{\Delta_w}\right)\right)e^{-i\vec{k}_w\cdot\vec{r}}\hat{\sigma}_{gg} - \frac{i}{\Delta_w}\left(1 - i\left(\frac{\gamma_{eg}}{\Delta_w}\right)\right)\hat{F}_{eg}. \tag{2.34}$$

By substituting these solutions (Eqs. 2.33–2.34) to Eq. 2.22, we obtain the effective interaction Hamilto-

[j]This is a reasonable approximation given that optical transitions correspond to a temperature scale $> 3,000$ K, relative to room-temperature 300 K.

nian (neglecting the noise terms and assuming constant atomic distribution $n_A(\vec{r}) = N_A/\mathcal{V}_1$)

$$\begin{aligned}\hat{H}_{\text{eff}}^{(\text{par})} &= \frac{N_A}{\mathcal{V}_1}\int d\vec{r}\left\{\hbar\Delta\hat{\sigma}_{ee}(\vec{r},t) - \hbar\delta\hat{\sigma}_{ss}(\vec{r},t) + \frac{\hbar|\Omega_w(\vec{r},t)|^2}{\Delta_w}\hat{\sigma}_{gg} - i\frac{\hbar|\Omega_w(\vec{r},t)|^2\gamma_{eg}}{\Delta_w^2}\hat{\sigma}_{gg}\right\} \\ &+\frac{1}{\mathcal{V}_1}\int d\vec{r}\left\{\hbar\chi_p(\vec{r},t;\Delta_w,\delta_{w1})\hat{\mathcal{E}}_1(\vec{r},t)\hat{\mathcal{S}}(\vec{r},t) + h.c.\right\}, \end{aligned} \tag{2.35}$$

where $\hat{\mathcal{S}}(\vec{r},t) = \sqrt{N_A}e^{-i(\vec{k}_w-\vec{k}_1)\cdot\vec{r}}\hat{\sigma}_{gs}(\vec{r},t)$ is the phase-matched slowly-varying spin-wave amplitude, and $\chi_p(\vec{r},t;\Delta_w,\delta_{w1}) \simeq g_p\sqrt{N_A}\frac{\Omega_w^*(\vec{r},t)}{\Delta_w - w_{gs}}$ is the effective parametric coupling constant. Here, the collective enhancement ($\sqrt{N_A}$) is manifested not by the increased emission rate of the Raman scattered photon, but by the increased quantum correlation between field 1 and collective excitation (section 2.4).

The first term of Eq. 2.35 includes the bare-state atomic Hamiltonian, light shift ($\sim \frac{\hbar|\Omega_w|^2}{\Delta_w}$), and the population loss of $\hat{\sigma}_{gg}$ due to optical pumping ($\sim \frac{i\hbar|\Omega_w|^2\gamma_{eg}}{\Delta_w^2}$). For our experiments, we can neglect the later two effects (optical pumping and light shift), as the intensity I_w for the write laser is well below the saturation intensity I_{sat} with a typical saturation parameter $s \equiv I_w/I_{\text{sat}} \equiv 2|\Omega_w|^2/\gamma_{eg}^2 \ll 10^{-4}$ (weak excitation limit). The second term, however, corresponds to a non-degenerate parametric amplification. This parametric matter-light interaction, denoted as

$$\hat{\mathcal{H}}_{\text{int}}^{(\text{par})}(t) = \hbar\left(\chi_p(t)\hat{\mathcal{E}}_1\hat{\mathcal{S}} + \chi_p^*(t)\hat{\mathcal{E}}_1^\dagger\hat{\mathcal{S}}^\dagger\right), \tag{2.36}$$

can generate a two-mode entangled state between the field 1 and the collective atomic mode via the squeezing operation $\hat{D} = \exp\left(-\frac{i}{\hbar}\int_0^\infty dt'\hat{\mathcal{H}}_{\text{int}}^{(\text{par})}(t')\right)$ (section 2.4).

2.3.2 Three-dimensional theory of spontaneous Raman scattering

Here, we derive a three-dimensional quantum theory of spontaneous Raman scattering by expanding the equations of motions in terms of the Hermite-Gaussian modes with mode indices (l,m). Under certain circumstance, we show that the 3D theory reduces an effective 1D model of a non-degenerate parametric amplifier between a single-mode (l,m) in field 1 and a single collective atomic mode (l,m).

2.3.2.1 Propagation equations of quantum fields and collective atomic variables

We start by deriving the equation of motion for the field $\vec{\hat{E}}_1^+(\vec{r},t)$ traveling along $\vec{k}_1 \parallel \hat{z}$ in the slowly-varying envelope approximation[143,170]. The wave equation for $\vec{\hat{E}}_1(\vec{r},t) = \vec{\hat{E}}_1^+(\vec{r},t)e^{-iw_1t} + \vec{\hat{E}}_1^-(\vec{r},t)e^{iw_1t}$ (Eq. 2.20) in a near-resonant atomic medium is given by

$$[\partial_t^2 - c^2\vec{\nabla}^2]\vec{E}_1(\vec{r},t) = -\frac{1}{\epsilon_0}\partial_t^2\vec{P}(\vec{r},t). \tag{2.37}$$

As in Eq. 2.20, we write the atomic polarization in terms of the slowly-varying atomic operator $\hat{\sigma}_{se}(\vec{r},t)$

$$\vec{\hat{P}}(\vec{r},t) = n_A(\vec{r})\left[d_{se}\vec{\epsilon}_{\rm a}\hat{\sigma}_{se}(\vec{r},t)e^{-i(\vec{k}_1\cdot\vec{r}-w_1t)} + h.c.\right]. \tag{2.38}$$

Assuming slowly-varying envelopes (i.e., $w_1\partial_t\mathcal{E}_1 \gg \partial_t^2\mathcal{E}_1$ and $w_1\hat{\sigma}_{se} \gg \partial_t\hat{\sigma}_{se}$), we then find the equation of motion for the slowly-varying amplitudes

$$\left[\partial_t - \frac{iw_1}{2}\left(1+\frac{\vec{\nabla}^2}{k_1^2}\right)\right]\mathcal{E}_1(\vec{r},t) = ig_pn_A(\vec{r})\mathcal{V}_1\hat{\sigma}_{se}(\vec{r},t)e^{-i\vec{k}_1\cdot\vec{r}}.$$

In the paraxial approximation, the quantized field propagates with the equation of motion

$$\left(\partial_t + c\partial_z - i\frac{c\vec{\nabla}_\perp^2}{2k_1}\right)\hat{\mathcal{E}}_1(\vec{r}_\perp,z,t) = ig_pn_A(\vec{r})\mathcal{V}_1\hat{\sigma}_{se}(\vec{r}_\perp,z,t)e^{-i\vec{k}_1\cdot\vec{r}}. \tag{2.39}$$

We can solve the coupled motions for the propagation of the atomic variables and the field 1 by substituting the adiabatic solutions $\hat{\sigma}_{es}, \hat{\sigma}_{ge}$ (Eq. 2.33) to the wave equation (Eq. 2.39) and to the Heisenberg-Langevin equation for the spin-wave variable $\hat{\sigma}_{gs}$ (Eq. 2.31), thereby yielding the following coupled differential equations (assuming a flat-top atomic number density $n_A(\vec{r}) = \frac{N_A}{\mathcal{V}_1}$)

$$\left(\partial_t + c\partial_z - \frac{ic\vec{\nabla}_\perp}{2k_1}\right)\hat{\mathcal{E}}_1(\vec{r},t) = i\chi_p(\vec{r},t;\Delta_w,\delta_{w1})\hat{\mathcal{S}}^\dagger(\vec{r},t) \tag{2.40}$$

$$\partial_t\hat{\mathcal{S}}(\vec{r},t) - \hat{F}_S = -\left(\frac{|\Omega_w|^2\gamma_{eg}}{\Delta_w^2} - i\delta'\right)\hat{\mathcal{S}}(\vec{r},t) + i\chi_p(\vec{r},t;\Delta_w,\delta_{w1})\hat{\mathcal{E}}_1^\dagger(\vec{r},t). \tag{2.41}$$

Here, we have assumed negligible spin-wave dephasing $\gamma_{gs} \simeq 0$ and $\delta' = \delta + \frac{|\Omega_w|^2}{\Delta_w}$, and $\hat{F}_S = \sqrt{N_A}e^{-i(\vec{k}_w-\vec{k}_1)\cdot\vec{r}}$ $\hat{F}_{gs}$ is the Langevin noise term for $\hat{\mathcal{S}}$.

2.3.2.2 Effective one-dimensional model

Here, I show that the three-dimensional Maxwell-Bloch equations (Eqs. 2.40–2.41) reduce to an effective 1D model for pencil-shaped ensembles (i.e., atomic Fresnel number $F_{\rm a} \simeq 1$) based on the formalism developed by Raymer *et al.* (ref.[70]). We assume a Gaussian write beam $\Omega_w(\vec{r},t) = \tilde{\Omega}_w(t)u_w(\vec{r}_\perp,z)$ with a mode function $u_w(\vec{r}_\perp,z)$ and $\chi_p(\vec{r},t;\Delta_w,\delta_{w1}) \simeq \chi_p'(t;\Delta_w,\delta_{w1})u_w(\vec{r}_\perp,z)$ (ref.[171]). We expand the quantum field $\hat{\mathcal{E}}_1(\vec{r},t)$ with Hermite-Gaussian modes $u_{lm}(\vec{r})$,

$$\hat{\mathcal{E}}_1(\vec{r},t) = \sum_{lm}\hat{\mathcal{E}}_{1,lm}(z,t)u_{lm}(\vec{r}) \tag{2.42}$$

$$\hat{\mathcal{S}}(\vec{r},t) = \sum_{lm}\hat{\mathcal{S}}_{lm}(z,t)u_{lm}(\vec{r}), \tag{2.43}$$

where the mode functions u_{lm} form a complete basis

$$\sum_{lm} u^*_{lm}(z,\vec{r}_\perp)u_{jk}(z,\vec{r}'_\perp) = \delta_{lj}\delta_{mk}\delta(\vec{r}_\perp - \vec{r}'_\perp), \tag{2.44}$$

and u_{lm} are the eigenfunctions for the paraxial equation $\left(\partial_z - \frac{i\vec{\nabla}_\perp}{2k_1}\right) u_{lm}(\vec{r}) = 0$ (see Eq. 2.40). Using these properties and formally integrating Eqs. 2.40–2.41 over $d\vec{r}_\perp$, we obtain the coupled equations of motions in terms of the mode functions

$$(\partial_t + c\partial_z)\hat{\mathcal{E}}_{1,lm}(z,t) = i\chi'_p \sum_{jk} \int d\vec{r}_\perp \left(u^*_{lm}(\vec{r})u_w(\vec{r})u_{jk}(\vec{r})\right) \hat{\mathcal{S}}^\dagger_{jk}(z,t) \tag{2.45}$$

$$\begin{aligned}\partial_t \hat{\mathcal{S}}_{jk}(z,t) &= -i\delta'\hat{\mathcal{S}}_{jk} - \frac{|\tilde{\Omega}_w|^2\gamma_{eg}}{\Delta_w^2} \sum_{lm} \int d\vec{r}_\perp \left(u^*_{jk}(\vec{r})|u_w(\vec{r})|^2 u_{lm}(\vec{r})\right) \hat{\mathcal{S}}_{lm} \\ &\quad + i\chi'^*_p \sum_{lm} \int d\vec{r}_\perp \left(u^*_{lm}(\vec{r})u_w(\vec{r})u_{jk}(\vec{r})\right) \hat{\mathcal{E}}^\dagger_{1,lm}.\end{aligned} \tag{2.46}$$

If we assume that the write beam ($u_w(z,\vec{r}_\perp)$) is much larger than the transverse dimension ($\vec{r}_\perp$) of the point-spread function for the imaging system of the field 1 ($u_{lm}(z,\vec{r}_\perp)$), such that $u_w(z,\vec{r}_\perp) \simeq u_w(z)$, then the integrals in Eqs. 2.45–2.46 reduce to $\int d\vec{r}_\perp \left(u^*_{lm}(\vec{r})u_w(z)u_{jk}(\vec{r})\right) \simeq \int d\vec{r}_\perp \left(u^*_{lm}(\vec{r})|u_w(z)|^2 u_{jk}(\vec{r})\right) \simeq \delta_{lj}\delta_{mk}$ (ref.[70,172]). In this case, the effective atomic density participating in the parametric interaction is defined by the field 1 mode, whose beam-waist is chosen to be much smaller than that of the write laser (pencil-shaped sample), and $F_{\rm a} = z_R/L \simeq 1$ (z_R is the Rayleigh range of field 1) in our experiment with $L \simeq z_R$. Thus, the resulting equations of motions are reduced to an effective 1D model with

$$(\partial_t + c\partial_z)\,\hat{\mathcal{E}}_{1,lm}(z,t) = i\chi_p(\vec{r},t;\Delta_w,\delta_{w1})\hat{\mathcal{S}}^\dagger_{lm}(z,t) \tag{2.47}$$

$$\partial_t \hat{\mathcal{S}}_{lm}(z,t) = -\left(\frac{|\Omega_w|^2\gamma_{eg}}{\Delta_w^2} - i\delta'\right)\hat{\mathcal{S}}_{lm}(z,t) + i\chi'^*_p(t)\hat{\mathcal{E}}^\dagger_{1,lm}(z,t) + \hat{F}_{lm}(z,t), \tag{2.48}$$

where $\hat{F}_{lm}(z,t)$ is the Langevin noise term associated with $\hat{\mathcal{S}}_{lm}$. The coupling between the creation of a single spin-wave $\hat{\mathcal{S}}^\dagger_{lm}(z,t)$ and the annihilation of a single photon $\hat{\mathcal{E}}_{1,lm}(z,t)$ in field 1 (and vice versa) in Eqs. 2.47–2.48 describes a non-degenerate parametric oscillator, which in turn generates a two-mode squeezed state between the collective atomic mode and the field 1 mode (section 2.4).

The spatio-temporal modes of $\hat{\mathcal{E}}_{1,lm}(z,t)$, $\hat{\mathcal{S}}_{lm}(z,t)$ and the normally ordered correlations such as : $\hat{\mathcal{S}}^\dagger_{lm}\hat{\mathcal{S}}_{lm}\hat{\mathcal{E}}^\dagger_{1,lm}\hat{\mathcal{E}}_{1,lm}$: can be derived from Eqs. 2.47–2.48. We will revisit some of the ideas developed here (section 2.5), whereby we solve the equation of motion for the retrieval process in the dark-state polariton picture[86,95,96]. I note that similar expressions have been derived in refs.[75,173]. More recently, optimal control theory has been applied to three-dimensional light scattering in a Λ-type ensemble[174].

2.4 Two-mode squeezed state as a quantum resource for *DLCZ* protocol

The initial atom-field state $|\overline{g}_{\rm a}, 0_{\gamma_1}\rangle$ in the Schrödinger's picture evolves to $|\Psi\rangle_{{\rm a}\gamma_1}$ via the unitary rotation $\hat{D} = \exp\left(-\frac{i}{\hbar}\int_0^\infty dt' \hat{\mathcal{H}}_{\rm int}^{\rm (par)}(t')\right)$ with the parametric interaction Hamiltonian $\hat{\mathcal{H}}_{\rm int}^{\rm (par)}$ (Eq. 2.36) derived in section 2.3.1.3. The final atom-field state ($t \to \infty$) is given by a two-mode squeezed state

$$|\Psi\rangle_{\gamma_1{\rm a}} = \sqrt{1-\xi}\sum \xi^{n/2}|n_{\gamma_1}, n_{\rm a}\rangle, \tag{2.49}$$

where $|n_{\gamma_1}\rangle$ ($|n_{\rm a}\rangle$) are the number-states for the photons $\sim (\hat{a}^\dagger)^n|0_{\gamma_1}\rangle$ (collective excitations $\sim (\hat{\mathcal{S}}^\dagger)^n|g_{\rm a}\rangle$) in field 1 (atomic ensemble), and $\xi = \tanh^2\left(i\int_0^\infty dt' \frac{1}{L}\int_0^L dz \chi_p(z,t')\right) \ll 1$ is the excitation parameter with the squeezing parameter given by $\chi_p(z,t;\Delta_w,\delta_{w1}) \simeq g_p\sqrt{N_A}\frac{\Omega_w^*(z,t)}{\Delta_w - w_{gs}}$. Additionally, we define for simplicity $\chi_p(t') = \frac{1}{L}\int_0^L dz \chi_p(z,t')$. For a rigorous treatment of dissipation and propagation effects, one needs to solve the self-consistent Heisenberg-Langevin equations in Eqs. 2.47–2.48, from which various correlation functions could be evaluated from Einstein's relations [143].

Here, we make several further remarks:

1. The mean photon number in field 1 is given by $\overline{n}_1 = {}_{\gamma_1{\rm a}}\langle\Psi|\hat{n}_1|\Psi\rangle_{\gamma_1{\rm a}} = \frac{\xi}{1-\xi}$ ($= \sinh(i\int_0^\infty dt' \chi_p(t'))$). Thus, the excitation probability $\xi = \frac{\overline{n}}{1+\overline{n}}$ follows the familiar thermal distribution. When the field 1 is traced over, the remaining atomic counterpart is equivalent to a thermal state where the ensemble exhibits super-Poissonian spin-wave statistics, $g^{(2)}(\tau) = \frac{\langle:\hat{n}_{\rm a}(t)\hat{n}_{\rm a}(t+\tau):\rangle}{|\langle\hat{n}_{\rm a}\rangle|^2} = 2$ (for $\tau = 0$).

2. For multiple ensembles and fields 1 (with the ensemble$\oplus$field 1 system labeled by $\alpha \in \{a, b, c, \cdots\}$), the overall state after the parametric Raman interaction is ideally $|\Psi\rangle_{\rm tot} = \prod_\alpha |\Psi\rangle_{\gamma_1{\rm a}}^{(\alpha)}$, where $|\Psi\rangle_{\gamma_1{\rm a}}^{(\alpha)} = \sqrt{1-\xi_\alpha}\sum \xi_\alpha^{n/2}|n_{\gamma_1}, n_{\rm a}\rangle_\alpha$.

3. In the ideal case, the conditional atomic state upon a photoelectric detection of a single field 1 photon on the mode $\hat{a}_{1,\alpha}$ is given by $\hat{\rho}_c = {\rm Tr}_1(\hat{a}_{1,\alpha}^\dagger \hat{a}_{1,\alpha}\hat{\rho}_{\gamma_1{\rm a}})$, where the initial atom-photon state prior to projection by $\hat{a}_{1,\alpha}^\dagger\hat{a}_{1,\alpha}$ is $\hat{\rho}_{\gamma_1{\rm a}} = |\Psi\rangle_{\gamma_1{\rm a}}^{(\alpha)}\langle\Psi|$.

4. The mode operators can be transformed nonlocally to $\hat{a}'_{1,\alpha} = \sum_{\alpha'} U_{\alpha,\alpha'}\hat{a}_{1,\alpha'}$ where $U_{\alpha,\alpha'}$ represents a unitary transformation of the mode operators $\hat{a}_{1,\alpha'}$. A photoelectric detection of a single photon in mode $\hat{a}'_{1,\alpha}$ leads to an effective interaction among the α' systems.

In section 2.5, we show that, after a delay τ, the collective excitation $\hat{\mathcal{S}}$ can be coherently mapped to another quantum field, called field 2 (with, ideally, unit probability) via the 'beamsplitter' transformation (Fig. 2.2b), with the dark-state polariton [86] $\hat{\Psi}_d(z,t) = \cos\theta(t)\hat{\mathcal{E}}_2(z,t) - \sin\theta(t)\hat{\mathcal{S}}(z,t)$ governing the matter-light evolution. When the atomic state is traced over, the matter-light transfer process is equivalent to replacing the collective operators $\hat{\mathcal{S}}$ and the state label, a, (indicating the atomic side of the Hilbert state) to $\hat{a}'_2 =$

$\sqrt{\eta_2}\hat{a}_2 + \sqrt{1-\eta_2}\hat{v}_2$ and a state label γ_2, respectively. Here, we account for the retrieval efficiency, the loss in the propagation and the detection of field 2 with a transmission efficiency η_2 in the beamsplitter transformation, where $\hat{v}_2$ is a vacuum mode operator[k]. Thus, ideally, we can transfer the two-mode squeezed state between an ensemble and field 1 to an equivalent state between fields 1 and 2,

$$|\Psi\rangle_{\gamma_1 \mathrm{a}} \mapsto |\Psi\rangle_{\gamma_1\gamma_2} = \sqrt{1-\xi}\sum \xi^{n/2}|n_{\gamma_1}, n_{\gamma_2}\rangle. \tag{2.50}$$

In practice, we control the excitation parameter $\xi = \tanh^2(i\int_0^\infty dt'\chi_p(t'))$ with the write intensity to modify the spin-wave statistics. For $\xi \gg 1$, the two modes contain significant *continuous-variable* entanglement, whereas in the regime of weak excitation $\xi \ll 1$, the two-mode squeezed state $|\Psi\rangle_{\gamma_1 \mathrm{a}}$ displays strong quantum correlations in the number-state basis. The field 2 and the field 1 can, indeed, exhibit strong non-classical correlations, as demonstrated experimentally in refs.[72,73], and be used as a critical resource for quantum information processing and communication[4]. Here, we calculate various intensity correlations between the fields 1 and 2, and obtain important benchmark parameters (used throughout the thesis), which characterize our experiments.

2.4.1 Two-mode squeezed state between an optical and collective atomic mode

The non-classical correlation between fields 1 and 2 can be verified by the violation of Cauchy-Schwarz inequality (refs.[170,175]),

$$R = \frac{|g_{12}|^2}{g_{11}g_{22}} \leq 1. \tag{2.51}$$

Here, we assume the initial state as the two-mode squeezed state $|\Psi\rangle_{\gamma_1\gamma_2}$ (Eq. 2.50). The normalized cross-correlation function g_{ij} between fields i, j is given by

$$g_{ij}(\tau) \equiv \frac{\langle : \hat{I}_i(t)\hat{I}_j(t+\tau) : \rangle}{\langle \hat{I}_i \rangle \langle \hat{I}_j \rangle}, \tag{2.52}$$

where $: \hat{\mathcal{O}} :$ indicates normally ordered operator for $\hat{\mathcal{O}}$. Here, $I_i = \eta_i \langle \hat{a}_i^\dagger \hat{a}_i \rangle$.

We obtain the following set of (auto- and cross-) intensity correlations,

$$\langle \Psi_{\gamma_2\gamma_1}| : \hat{I}_i : |\Psi_{\gamma_1\gamma_2}\rangle = \eta_i \frac{\xi}{1-\xi} = \overline{n}_i \tag{2.53}$$

$$\langle \Psi_{\gamma_2\gamma_1}| : \hat{I}_1\hat{I}_2 : |\Psi_{\gamma_1\gamma_2}\rangle = \eta_1\eta_2 \frac{\xi(1+\xi)}{(1-\xi)^2} \tag{2.54}$$

$$\langle \Psi_{\gamma_2\gamma_1}| : \hat{I}_i^2 : |\Psi_{\gamma_1\gamma_2}\rangle = \eta_i^2 \frac{2\xi^2}{(1-\xi)^2}, \tag{2.55}$$

[k] To include noise, we can add mixed coherent states $|v_i\rangle$ on a reservoir mode $\hat{v}_i$ entering the system $\hat{a}_i$ (see the supplementary information of ref.[33], chapter 9).

where we obtain normalized auto-correlation functions $g_{ii} = 2$ for $i \in \{1, 2\}$, and a cross-correlation

$$g_{12} = 1 + \frac{1}{\xi}. \tag{2.56}$$

Thus, we observe the presence of strong quantum correlations between the fields 1 and 2 by way of the violation of Cauchy-Schwarz inequality $R = \frac{1}{4}\left(1 + \frac{1}{\xi}\right)^2 = \frac{g_{12}^2}{4} \not\leq 1$ for $\xi < 1$ ($g_{12} > 2$). Since the initial experiments[72,73], the Cauchy-Schwarz inequality has been violated by a factor up to $R \geq 10^5$ by the group of Steve Harris in a 2D magneto-optical trap[81].

2.4.2 Heralded single-photon source

In the single-excitation regime $\xi \ll 1$, the initial two-mode squeezed state between the ensemble and field 1 can be expanded as

$$|\Psi\rangle_{\gamma_1 \mathrm{a}} \simeq |0_{\gamma_1}, 0_{\mathrm{a}}\rangle + \sqrt{\xi}|1_{\gamma_1}, 1_{\mathrm{a}}\rangle + \mathcal{O}(\xi). \tag{2.57}$$

A measurement of a single photon in field 1 ($: \hat{I}_1 :$) projects the remaining ensemble counterpart to a state of (ideally) single collective excitation $\hat{\rho}_c = \mathrm{Tr}_{\gamma_1}(: \hat{I}_1 : |\Psi\rangle_{\gamma_1 \mathrm{a}}\langle\Psi|)$. After a controllable delay τ, we map the single excitation to a single photon $|\Psi\rangle_{\gamma_1 \mathrm{a}} \mapsto |\Psi\rangle_{\gamma_1 \gamma_2}$ (ref.[74]). Thus, a probabilistic detection of a single photon in field 1 heralds (signals) the creation of single collective excitation, which we subsequently transfer to a single photon in a triggered fashion.

We characterize the quality of the heralded single-photon source with the conditional auto-correlation function $g_c^{(2)}$, also denoted by $w = \frac{p_{11}}{p_{10}p_{01}}$, in a Hanbury Brown-Twiss setup[176,177]. Here, the p_{ij} are the conditional probabilities to detect i, j photons in two respective detectors measuring the two modes $\hat{a}_{2,a}, \hat{a}_{2,b}$ after a beamsplitter. The transformed mode operators are given by

$$\begin{aligned} \hat{a}_{2,a} &= \frac{1}{\sqrt{2}}\left(\hat{a}_2 + \hat{v}_2\right) \\ \hat{a}_{2,b} &= \frac{1}{\sqrt{2}}\left(\hat{a}_2 - \hat{v}_2\right). \end{aligned}$$

Using these mode operators, we calculate the intensity correlations (with $i \in \{2a, 2b\}$)

$$\langle : \hat{I}_1 \hat{I}_{2a} \hat{I}_{2b} : \rangle = \eta_1 \eta_{2a} \eta_{2b} \frac{\xi^2(2+\xi)}{2(1-\xi)^3} \tag{2.58}$$

$$\langle : \hat{I}_1 \hat{I}_i : \rangle = \eta_1 \eta_i \frac{\xi(1+\xi)}{2(1-\xi)^2}, \tag{2.59}$$

for which we obtain a suppression of higher-order excitations (and non-classical photon statistics) relative to that of a coherent state

$$w = \frac{\langle : \hat{I}_1 \hat{I}_{2a} \hat{I}_{2b} : \rangle \langle : \hat{I}_1 : \rangle}{\langle : \hat{I}_1 \hat{I}_{2a} : \rangle \langle : \hat{I}_1 \hat{I}_{2b} : \rangle} = \frac{4\xi}{(1+\xi)^2} + \frac{2\xi^2}{(1+\xi^2)^2} \simeq \frac{4}{g_{12}}. \tag{2.60}$$

We compare our result of w (Eq. 2.60) to coherent states $|\alpha\rangle$, a minimum uncertainty state that defines the quantum-classical boundary[170], $w_b = \langle :\hat{n}^2: \rangle / |\langle \hat{n} \rangle|^2 = |\alpha|^4/|\alpha|^4 = 1$ (for fields with Poissonian statistics). Thus, we obtain non-classical sub-Poissonian photon statistics $w < w_b = 1$ for $g_{12} \gtrsim 4$ (in contrast to the super-Poissonian statistics $g^{(2)}(0) = 2$ of the fields 1 and 2 when taken alone).

2.4.3 Measurement-induced entanglement

Having established the presence of quantum correlations between the number states of the field 1 and the collective excitation, we show that entanglement between two atomic ensembles can be created by a path-erasing measurement of a single photon (field 1) emitted indistinguishably from the two ensemble.

Specifically, we start from a pair of two-mode squeezed states (Eq. 2.49)

$$
\begin{aligned}
|\Psi\rangle_{\text{tot}} &= |\Psi\rangle^{(L)}_{\gamma_1 \text{a}} \otimes |\Psi\rangle^{(R)}_{\gamma_1 \text{a}} && (2.61)\\
&\simeq \sqrt{(1-\xi_L)(1-\xi_R)} \left(|0_{\gamma_1}, \overline{g}_{\text{a}}\rangle_L + \sqrt{\xi}_L e^{i\phi_L} |1_{\gamma_1}, \overline{s}_{\text{a}}\rangle_L + \mathcal{O}(\xi_L) \right) \\
&\quad \otimes \left(|0_{\gamma_1}, \overline{g}_{\text{a}}\rangle_R + \sqrt{\xi}_R e^{i\phi_R} |1_{\gamma_1}, \overline{s}_{\text{a}}\rangle_R + \mathcal{O}(\xi_R) \right) && (2.62)
\end{aligned}
$$

by illuminating the two atomic ensembles, L and R, with Ω_w. The relative phase ϕ_w between the two writing beams is given by $\phi_w = \phi_L - \phi_R$, where $\phi_{L,R}$ are the phases associated with the writing lasers illuminating ensembles L, R. A photoelectric detection $\hat{I}_{1,l} = \eta_l \hat{a}^\dagger_{1,l} \hat{a}_{1,l}$ (or $\hat{I}_{1,r} = \eta_r \hat{a}^\dagger_{1,r} \hat{a}_{1,r}$) of a single photon in field 1 after a beamsplitter projects the initial quantum state of ensemble-field system $|\Psi\rangle_{\text{tot}}$, where the mode operators for the output ports $\{l, r\}$ of the beamsplitter ($\cos(\theta_1) : \sin(\theta_1)$ ratio) are given by

$$
\begin{aligned}
\hat{a}_{1,l} &= \cos\theta_1 \hat{a}_{1,L} + e^{i\phi_1} \sin\theta_1 \hat{a}_{1,R} \\
\hat{a}_{1,r} &= -\sin\theta_1 \hat{a}_{1,L} + e^{-i\phi_1} \cos\theta_1 \hat{a}_{1,R}.
\end{aligned}
$$

The conditional atomic states upon the probabilistic photoelectric events $\hat{I}_{1,l}$ and $\hat{I}_{1,r}$ are given by

$$
\begin{aligned}
\hat{\rho}^{(l)}_{\text{ent}} &= \frac{\text{Tr}_1(\hat{I}_{1,l} \hat{\rho}_{\gamma_1 \text{a}})}{\langle \hat{I}_{1,l} \rangle} = |\Psi\rangle^{(l)}_{\text{tot}} \langle \Psi| && (2.63)\\
\hat{\rho}^{(r)}_{\text{ent}} &= \frac{\text{Tr}_1(\hat{I}_{1,r} \hat{\rho}_{\gamma_1 \text{a}})}{\langle \hat{I}_{1,r} \rangle} = |\Psi\rangle^{(r)}_{\text{tot}} \langle \Psi|. && (2.64)
\end{aligned}
$$

Thus, we obtain heralded entanglement between the two atomic ensembles,

$$
|\Psi\rangle^{(l)}_{\text{tot}} \simeq \left(\sqrt{\frac{\xi_R}{\xi_{\text{tot}}}} \sin\theta_1 |\overline{g}_{\text{a},L}, \overline{s}_{\text{a},R}\rangle + e^{i(\phi_w - \phi_1)} \sqrt{\frac{\xi_L}{\xi_{\text{tot}}}} \cos\theta_1 |\overline{s}_{\text{a},L}, \overline{g}_{\text{a},R}\rangle \right) + \mathcal{O}(\sqrt{\xi}_{L,R}) \quad (2.65)
$$

$$
|\Psi\rangle^{(r)}_{\text{tot}} \simeq \left(\sqrt{\frac{\xi_R}{\xi_{\text{tot}}}} \cos\theta_1 |\overline{g}_{\text{a},L}, \overline{s}_{\text{a},R}\rangle - e^{-i(\phi_w - \phi_1)} \sqrt{\frac{\xi_L}{\xi_{\text{tot}}}} \sin\theta_1 |\overline{s}_{\text{a},L}, \overline{g}_{\text{a},R}\rangle \right) + \mathcal{O}(\sqrt{\xi}_{L,R}), \quad (2.66)
$$

where $\xi_{\text{tot}} = \xi_L + \xi_R$ is the total excitation probability.

The degree of entanglement is characterized by concurrence [178], a monotonic function of entanglement [27],

$$C \simeq \max(Vp_1 - 2\sqrt{p_0 p_{11}}, 0) \geq \max(p_1(V - \sqrt{p_0 h_c}), 0), \tag{2.67}$$

where the two-photon contamination for the global joint state of the two ensembles and off-diagonal coherence are characterized by a normalized parameter $h_c \equiv \frac{p_{11}}{p_{10}p_{01}} \simeq 4/g_{12}$ and by $d = Vp_1/2$ (chapter 3). Here, $V = \frac{\max(\langle \hat{I}_{2,l} \rangle) - \min(\langle \hat{I}_{2,l} \rangle)}{\max(\langle \hat{I}_{2,l} \rangle) + \min(\langle \hat{I}_{2,l} \rangle)} \simeq \frac{g_{12}-1}{g_{12}+1}$ (assuming $\xi_L = \xi_R$ and $\theta_1 = \pi/4$) is the visibility for the interference between the two fields $2_L, 2_R$ retrieved from $\hat{\rho}_{\text{ent}}^{(l,r)}$ (chapter 3), with the mode operators defined as

$$\begin{aligned} \hat{a}_{2,l} &= \frac{1}{\sqrt{2}} \left(\hat{a}_{2,L} + e^{i\phi_2} \hat{a}_{2,R} \right) \\ \hat{a}_{2,r} &= \frac{1}{\sqrt{2}} \left(-\hat{a}_{2,L} + e^{-i\phi_2} \hat{a}_{2,R} \right). \end{aligned}$$

A necessary condition for entanglement is $h_c \simeq 4/g_{12} < 1$ (for independent coherent states $|\alpha_1, \alpha_2\rangle$, $h_c = 1$). A similar quantity $y_c \equiv \frac{4p_{11}p_0}{p_1^2}$ is derived in the language of quantum uncertainty (Δ) relations (chapters 7–9), where $C = \max\left(p_1\left(\sqrt{1-2\Delta} - \sqrt{y_c}\right), 0\right)$.

2.5 Collective atom-light interaction

The dynamics of N_A Λ-level atoms dressed by applied laser fields determines the optical response of the coherent atomic medium. In addition to the Dicke-like superradiant emission (section 2.2), the coherent manipulation of dark resonances[94,179–184] enables a robust and efficient method of transferring quantum states[185] between photons and spin waves in a matter-light quantum interface. Closely connected to classical coherent phenomena of coherent population trapping[179,183] (CPT) and stimulated Raman adiabatic transfer[180,181,184] (STIRAP), a dark-state polariton is a half photonic and half matter quasi-particle excitation, proposed by Michael Fleischhauer and Mikhail Lukin[86,87], which describes low-light level electromagnetically induced transparency[94,182] (EIT). Coherent preparation and control of EIT at the single-photon level are utilized in many experiments, including those in my thesis, for the coherent transfer of heralded spin-waves (section 2.3, Fig. 2.2a) to single photons (chapters 3–5 and 9, Fig. 2.2b) and for the reversible mapping of a photonic entanglement into and out of quantum memories (chapter 6, Fig. 2.3).

Stated explicitly, the dark-state polariton $\hat{\Psi}_d(z,t) = \cos\theta_d(t)\hat{\mathcal{E}}_s(z,t) - \sin\theta_d(t)\hat{\mathcal{S}}(z,t)$ is a coherent superposition state of electromagnetic and spin-wave excitations and is a quantum analogue of the classic dark state in CPT[179,183,184]. The adiabatic following of $\hat{\Psi}_d$ with respect to the rotation of mixing angle θ_d leads to a reversible and (ideally) complete transfer between quantum optical states $\hat{\mathcal{E}}_s(z,t)$ and spin-waves $\hat{\mathcal{S}}(z,t)$ without dissipation via *dynamic* EIT. Here, we theoretically analyze the operation of our quantum interface in this polaritonic picture. In chapter 6, we provide a semi-classical picture to the observations of *static* EIT and CPT, and the connections to the polaritonic picture discussed here. There, we discuss the technical considerations towards *dynamic* EIT (such as the importance of Zeeman populations in a multi-level system). In chapter 6, we also present a numerical optimization scheme for improving the storage and retrieval efficiency based on the works by Gorshkov *et al.*[186–189].

Following the method developed in section 2.3, we treat quantum mechanically the propagation and the dynamics of the coupled motions of the quantum fields (called the signal field ($\hat{\mathcal{E}}_s$), or the field 2 ($\hat{\mathcal{E}}_2$)) and the collective excitations in an EIT media. For simplicity, we call $\hat{\mathcal{E}}_s$ the quantum field of interest for storage and/or retrieval, whether it is externally provided from an offline source (signal field) or generated internally from the parametric interaction (field 2). Based on the results in section 2.3, we use an effective 1D model[86,87]. We show that the signal field's group velocity v_g can be dynamically controlled by an external control laser $\Omega_c(z,t)$ from the free-space velocity $v_g = c$ to ultraslow group velocities $v_g \ll c$ and to a complete halt $v_g = 0$ (coherent storage) for the quantum field (and vice versa). In particular, we find that dark-state polaritons $\hat{\Psi}_d$ can be dynamically decelerated and accelerated while preserving the phase-amplitude information of the quantum field $\hat{\mathcal{E}}_s$ by transferring to and from stationary collective excitations $\hat{\mathcal{S}}$.

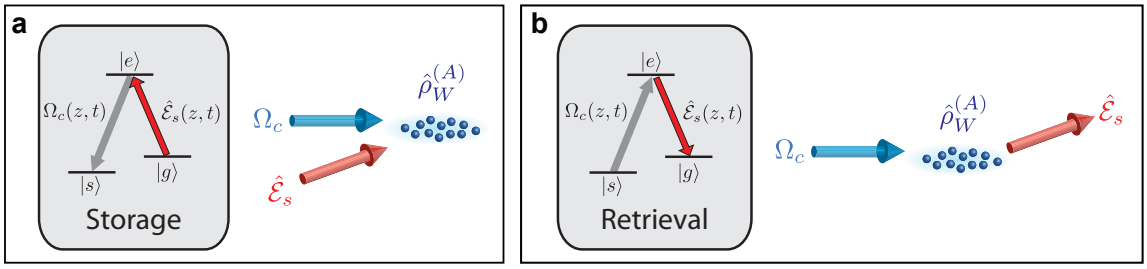

Figure 2.3: **Reversible matter-light quantum interface via dark-state polariton. a**, Mapping single photons to single collective excitations. A strong resonant control laser ($|e\rangle \rightarrow |s\rangle$ transition) with Rabi frequency $\Omega_c(z,t)$ is illuminated onto the ensemble in a counter-intuitive order[181], thereby preparing $|g\rangle$ as the dark-state. As the weak quantum field $\hat{\mathcal{E}}_s$ ($|g\rangle \rightarrow |e\rangle$ transition), called the signal field, enters the coherent atomic medium, the control laser is adiabatically turned off, thereby storing the quantum state of $\hat{\mathcal{E}}_s$ in the collective atomic excitation $\hat{\mathcal{S}}(z,t)$. **b**, Mapping single collective excitations to single photons. After a delay τ, the intensity of the control laser is adiabatically increased, thereby transferring the then dark-state $|\overline{s}\rangle$ back to the signal field $\hat{\mathcal{E}}_s$. The signal field $\hat{\mathcal{E}}_s$ propagates within the EIT window of the ensemble, provided by $\Omega_c(z,t)$.

2.5.1 Interaction Hamiltonian and formation of dark states

Here, we consider a collection of Λ-level atoms interacting with the two single-mode optical fields. The transition $|g\rangle - |e\rangle$ of each of these atoms is coupled to a slowly-varying quantized radiation mode $\hat{\mathcal{E}}_s$ (with two-photon detuning δ), called the signal field, whereas the transition $|s\rangle - |e\rangle$ is resonantly driven by a classical control field of Rabi frequency Ω_c (with detuning Δ_c). The dynamics of this system is described by the Hamiltonian $\hat{H}_s^{(\text{map})}$ in the rotating-wave approximation (following the effective one-dimensional approximation in section 2.3.2.2 and neglecting the transverse profiles), with

$$\begin{aligned}\hat{H}_s^{(\text{map})} &= \int dw \hbar w \hat{a}_w^\dagger \hat{a}_w + \sum_{i=1}^{N_A} \left(\hbar w_{es} \hat{\sigma}_{ss}^{(i)} + \hbar w_{eg} \hat{\sigma}_{gg}^{(i)} \right) \\ &\quad \underbrace{- \sum_{i=1}^{N_A} \left(\hbar \Omega_c \hat{\sigma}_{es}^{(i)} e^{i(k_c^{\parallel} z_i - w_c t)} + d_{eg} \hat{\sigma}_{eg}^{(i)} \vec{\epsilon}_{\text{a}} \cdot \vec{\hat{E}}_s^{+} e^{i(k_s z_i - w_s t)} + h.c. \right)}_{\hat{H}_{\text{int}}^{(\text{map})}}, \end{aligned} \tag{2.68}$$

where $\vec{\hat{E}}_s^{+} = i\sqrt{\frac{\hbar w_s}{2\epsilon_0 \mathcal{V}}} \int dw \hat{a}_w e^{iwz/c} \vec{\epsilon}_s$ is the positive frequency component of the signal field, and $k_c^{\parallel} = \vec{k}_c \cdot \hat{z}$ is the longitudinal projection of the wave-vector along $\hat{z}$ (also, $k_c^{\perp} = |\vec{k}_c \cdot (\hat{x}, \hat{y})| \simeq 0$). We assumed that the signal field propagates along the quantization axis $\hat{z}$ of the system (section 2.3.2.2).

A simple explanation for the formation of dark-state polariton is the existence of a family of dark eigenstates $|D, m\rangle$ for the interaction Hamiltonian $\hat{H}_{\text{int}}^{(\text{map})}$ (ref.[87]). In particular, the single-excitation state $|D, m = 1\rangle$ is (ref.[87])

$$|D, 1\rangle = \cos\theta_d(t) |\overline{g}_{\text{a}}, 1_s\rangle - \sin\theta_d(t) |\overline{s}_{\text{a}}, 0_s\rangle, \tag{2.69}$$

where $\tan\theta_d = g_d\sqrt{N_A}/\Omega_c$ defines the mixing angle, $g_d = i d_{eg}\sqrt{\frac{w_s}{2\hbar\epsilon_0 \mathcal{V}}}$ $(\vec{\epsilon}_{eg} \cdot \vec{\epsilon}_s)$ is the single atom-

photon coupling constant[1], $|n_s\rangle$ is the Fock state for the signal field, $|\overline{s}\rangle_{\rm a} = \frac{1}{\sqrt{N_A}}\sum_{i=1}^{N_A} e^{-i\Delta k_{sc} z_i}\hat{\sigma}_{gs}^{(i)\dagger}|\overline{g}\rangle_{\rm a}$ is the collective spin excitation (see section 2.3.1.1), and $\Delta k_{sc} = k_s - k_c^{\parallel}$ is the momentum transfer to the spin waves (section 2.6). Since these dark states do not contain the excited state $|e\rangle$, they are immune to spontaneous emission[185]. The collective dark states provide a robust method of mapping a weak quantum field $\hat{\mathcal{E}}_s(z,t)$ to and from collective atomic excitations $\hat{\mathcal{S}}(z,t)$ via the adiabatic rotations of $\theta_d = 0 \leftrightarrow \pi/2$ (i.e., by controlling $\Omega_c(z,t)$).

2.5.2 Heisenberg-Langevin equations

As in section 2.3.1.1, we express the system Hamiltonian $\hat{H}_s^{(\rm map)}$ with slowly-varying operators (Eqs. 2.20 and 2.23) in the limit of continuum along $\hat{z}$ (i.e., $\sum_i \rightarrow \int_0^L n_A(z)dz$) and in the rotating frame,

$$\begin{aligned}\hat{H}_s^{(\rm map)} &= \int_0^L dz n_A(z)\{\hbar\Delta_c\hat{\sigma}_{ee}(z,t) - \hbar\delta\hat{\sigma}_{ss}(z,t) \\ &\quad - \underbrace{\left[\hbar g_d\hat{\mathcal{E}}_s(z,t)e^{ik_s z}\hat{\sigma}_{eg}(z,t) + \hbar\Omega_c(z,t)e^{ik_c z}\hat{\sigma}_{es}(z,t) + h.c.\right]}_{\hat{H}_{\rm int}^{(\rm map)}}\},\end{aligned} \tag{2.70}$$

where $n_A(z)$ is the linear atomic density ($\int dz n_A(z) = N_A$).

Following the Heisenberg-Langevin approach (Eq. 2.29), we obtain a set of differential equations governing the atomic evolutions (assuming weak signal field approximation $g_d \ll \Omega_c$ and $\overline{n}_s \ll N_A$)

$$\partial_t\hat{\sigma}_{se} = -(\gamma_{se} + i(\Delta_c - w_{gs}) - i\delta)\hat{\sigma}_{se} + i\Omega_c e^{i(k_c^{\parallel}-k_s)z}(\hat{\sigma}_{ss} - \hat{\sigma}_{ee}) + ig_d\hat{\mathcal{E}}_s\hat{\sigma}_{ge} + \hat{F}_{se} \tag{2.71}$$

$$\partial_t\hat{\sigma}_{gs} = -\gamma_{gs}\hat{\sigma}_{gs} + i\Omega_c^* e^{-i(k_c^{\parallel}-k_s)z}\hat{\sigma}_{ge} - ig_d\hat{\mathcal{E}}_s\hat{\sigma}_{es} + \hat{F}_{gs} \tag{2.72}$$

$$\partial_t\hat{\sigma}_{ge} = -(\gamma_{ge} + i\Delta_c)\hat{\sigma}_{ge} + i\Omega_c e^{i(k_c^{\parallel}-k_s)z}\hat{\sigma}_{gs} + ig_d\hat{\mathcal{E}}_s(\hat{\sigma}_{gg} - \hat{\sigma}_{ee}) + \hat{F}_{ge}, \tag{2.73}$$

and a propagation equation for the quantum field $\hat{\mathcal{E}}_s(z,t)$ in an effective one-dimension (Eq. 2.39),

$$(\partial_t + c\partial_z)\,\hat{\mathcal{E}}_s(z,t) = ig_d n_A(z)L\hat{\sigma}_{ge}(z,t). \tag{2.74}$$

Here, $\hat{F}_{\mu\nu}$ are the quantum Langevin operators for the atomic operators $\hat{\sigma}_{\mu\nu}$, as described in section 2.3.

2.5.2.1 Weak field approximation and adiabatic condition

In the weak signal field approximation with g_d ($\sigma_{gg} \simeq 1 \gg \sigma_{ee}, \sigma_{ss}, \sigma_{es} \simeq 0$) and with negligible spin-wave dephasing $\gamma_{gs} \simeq 0$ over the interaction time δt_c, we approximate $\hat{\sigma}_{ge} = -i\left(e^{i(k_c^{\parallel}-k_s)z}/\Omega_c^*\right)\partial_t\hat{\sigma}_{gs}$ (Eq.

[1] $\vec{\epsilon}_{eg}$ and $\vec{\epsilon}_s$ are the respective polarization vectors for the atomic dipole ($|g\rangle - |e\rangle$ transition) and the signal field.

2.72) and obtain the coupled equations of motions (by substituting $\hat{\sigma}_{ge}$ into Eq. 2.74, and using Eq. 2.73)

$$(\partial_t + c\partial_z)\,\hat{\mathcal{E}}_s(z,t) \simeq \frac{g_d n_A(z) L}{\Omega_c^*(z,t)} e^{i(k_c^{\parallel}-k_s)z}\partial_t\hat{\sigma}_{gs} \tag{2.75}$$

$$\hat{\sigma}_{gs} \simeq -\frac{g_d\hat{\mathcal{E}}_s}{\Omega_c}e^{-i(k_c^{\parallel}-k_s)z} \underbrace{-\frac{\gamma_0}{|\Omega_c|^2}\partial_t\hat{\sigma}_{gs} - \frac{1}{|\Omega_c|^2}\partial_t^2\hat{\sigma}_{gs}}_{\text{(Non-adiabatic terms)}} + i\frac{e^{-i(k_c^{\parallel}-k_s)z}}{\Omega_c}\hat{F}_{ge}, \tag{2.76}$$

where $\gamma_0 = \gamma_{ge} + i\Delta_c$.

In the adiabatic condition[86,190,191] ($\frac{\partial_t\Omega_c}{\Omega_c} \sim \frac{1}{\delta t_c} \ll \gamma_{ge}\tilde{d}_0(L)$ with resonant optical depth given by $\tilde{d}_0(z) = \int_0^z dz' \frac{2g_d^2 n_A(z')z}{\gamma_{ge}c}$), we perturbatively expand Eq. 2.76 to the order of $\partial_t\hat{\mathcal{O}} \sim \hat{\mathcal{O}}/\delta t_c$, and we obtain the lowest-order perturbation $\hat{\sigma}_{gs} \simeq -\frac{g_d\hat{\mathcal{E}}_s}{\Omega_c}e^{-i(k_c^{\parallel}-k_s)z}$. Thus, we obtain the adiabatic equation of motion for the quantum field $\hat{\mathcal{E}}_s(z,t)$

$$(\partial_t + c\partial_z)\,\hat{\mathcal{E}}_s(z,t) \simeq \frac{g_d^2 n_A(z) L}{\Omega_c^*(z,t)}\frac{\partial}{\partial t}\left(\frac{\hat{\mathcal{E}}_s(z,t)}{\Omega_c(z,t)}\right). \tag{2.77}$$

We note that the characteristic pulse widths $\delta t_c \simeq 10$ ns of the control laser (or the read laser) in our experiments are on the same order of magnitude as the adiabatic criteria $1/\delta t_c \simeq \gamma_{ge}\tilde{d}_0(L)$, where the resonant transmission (absent the control laser) is defined as $T_0 = e^{-\tilde{d}_0(L)}$. Thus, instead of the simplified wave equation (Eq. 2.77), we numerically solve the coupled differential equations of motions (Eqs. 2.71–2.74) in chapter 6.

2.5.2.2 Coherent atomic medium and EIT

In Eq. 2.77, we recover the usual wave equation with slow-light phenomena in *static* EIT (with static control field $\Omega_c(z,t) = \Omega_c$) with modified group velocity $v_g = c\cos^2\theta_d$. Furthermore, if there is very little population in $\hat{\sigma}_{ss}$ and $\hat{\sigma}_{se}$, the control field $\Omega_c(z,t) \simeq \Omega_c(t - z/c)$ propagates according to the free-space wave equation ($(\partial_t + c\partial_z)\,\Omega_c(z,t) = 0$). In this case, we obtain a wave equation with variable group velocity $v_g(z,t)$; namely,

$$\left(\frac{\partial}{\partial t} + v_g(z,t)\frac{\partial}{\partial z}\right)\hat{\mathcal{E}}_s(z,t) = 0, \tag{2.78}$$

where the group velocity $v_g(z,t) = c\cos^2\theta_d(z,t)$ is dynamically controlled by the Rabi frequency $\Omega_c(z,t)$ of the control laser. Here, the mixing angle is given by $\cos\theta_d = \frac{\Omega_c}{\sqrt{g_d^2 N_A + \Omega_c^2}}$ for constant density $n_A = N_A/L$.

We now briefly turn to a more classic situation encountered in EIT (see also chapter 6). For a resonant control field with $\Delta_c = 0$, the EIT medium behaves as a non-absorbing dispersive media within the transparency window given by Ω_c at the two-photon resonance $\delta = 0$ shown in Fig. 2.4. The adiabatic approximation in section 2.5.2.1 in essence compares the pulse bandwidth to the EIT window Ω_c. If the pulse bandwidth $\Delta w_s \simeq 2\pi/\delta t_c \simeq \Omega_c$, higher-order dispersion must be taken into account. Specifically, the

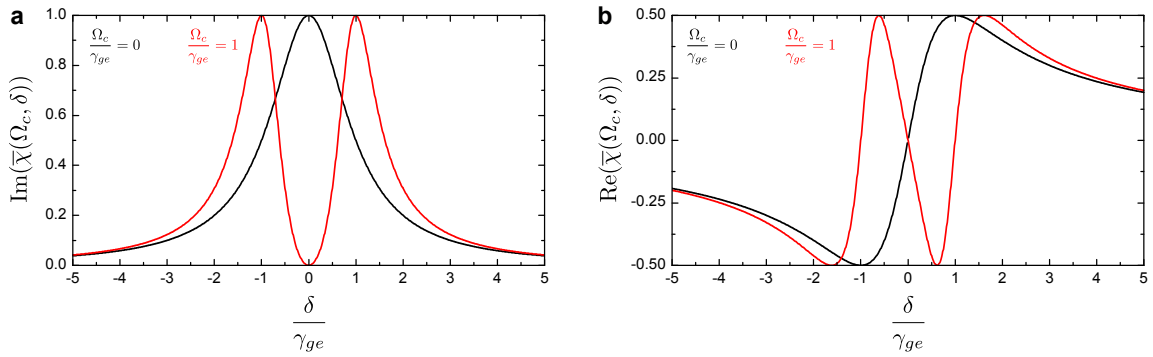

Figure 2.4: **Susceptibility $\overline{\chi}_s$ of EIT medium.** **a**, Imaginary part of the susceptibility function, $\mathrm{Im}(\overline{\chi}_s(\Omega_c,\delta))$. **b**, Real part of the susceptibility function $\mathrm{Re}(\overline{\chi}_s(\Omega_c,\delta))$. We show the dispersions of the EIT medium (red line) with a control laser Rabi frequency $\Omega_c/\gamma_{ge}=1$, as well as for the bare atomic medium (black line) with $\Omega_c=0$. Dynamic control of the group velocity (i.e., $v_g=\frac{c}{1+(w_{eg}-\delta)dn/d\delta}$ at $\delta=0$) allows shape-preserving acceleration/deceleration of the signal field in the presence of transparency $\mathrm{Im}(\overline{\chi}_s)\simeq 0$ at $\delta=0$.

susceptibility χ_s of the signal field in a homogeneous EIT medium (defined as $\mathcal{P}(z,t)=\epsilon_0\chi_s\mathcal{E}_s(z,t)$) for a resonant control field ($\Delta_c=0$) is given by (refs.[94,143])

$$\chi_s=\frac{2g_d^2N_A}{w_s}\overline{\chi}_s, \tag{2.79}$$

where $\overline{\chi}_s=\frac{\delta}{|\Omega_c|^2-\delta^2-i\gamma_{ge}\delta}$ is the normalized susceptibility function and $\mathcal{P}(z,t)=\sqrt{N_A}\hat{\sigma}_{ge}$ is the atomic polarization. $\mathrm{Im}(\overline{\chi}_s(\Omega_c,\delta))$ describes the transparency for the signal field at $\delta=0$ with the transmission given by $T(\Omega_c,\delta)=\exp\left(-k_sL\mathrm{Im}(\chi_s)\right)=\exp\left(-\tilde{d}_0\mathrm{Im}(\overline{\chi}_s)\right)$ (Fig. 2.4a), whereas $\mathrm{Re}(\overline{\chi}_s(\Omega_c,\delta))$ contributes to the refractive index $n_s(\delta)=\sqrt{1+\mathrm{Re}(\chi_s)}$ for the signal field (group velocity given by $v_g=\frac{c}{1+(w_{eg}-\delta)dn/d\delta}$) (Fig. 2.4b)[m].

Perturbatively expanding χ_s (Eq. 2.79) around $\frac{\delta}{\Omega_c}\ll 1$, we find $\chi_s\simeq\frac{2g_d^2N_A}{w_s}\left(\frac{\delta}{|\Omega_c|^2}+i\frac{\delta^2\gamma_{eg}}{|\Omega_c|^4}+\mathcal{O}(\delta^3)\right)$, where the linear dispersion gives $v_g=c\cos^2\theta_d$. In addition, we find the bandwidth of the EIT medium via $T\simeq\exp(-\delta^2/\Delta w_{\mathrm{EIT}}^2)$, where the EIT bandwidth is $\Delta w_{\mathrm{EIT}}=\frac{|\Omega_c|^2}{\gamma_{eg}\sqrt{\tilde{d}_0}}$. This leads to an adiabatic condition, where the initial signal pulse's bandwidth Δw_s must be smaller than the bandwidth of the EIT medium Δw_{EIT}: i.e., $\Delta w_s<\Delta w_{\mathrm{EIT}}$. In addition, the adiabatic passage of the dark-state polariton[192] sets a limit to the rotation speed of the mixing angle θ_d of the polariton $\hat{\Psi}_d(z,t)$[n]. Introducing a characteristic time-scale δt_c, we obtain the criteria $\delta t_c>\frac{\gamma_{eg}v_g}{g_d^2N_Ac}$ for adiabatic following[86]. Finally, I note that we have so far neglected the presence of Zeeman population and assumed an ideal Λ-level system. In fact, the distribution of Zeeman populations can inhibit the presence of EIT unless a special polarization scheme is employed (chapter 6).

[m] More generally, the "transfer" function of the signal field in the EIT medium is given by $t(\Omega,\delta,z)=\exp(ikz\chi_s/2)$, where the transmission is $T=|t|^2$.

[n] In fact, the rotation speed $\dot{\theta}_d$ of the mixing angle is proportional to the transition rate between $\hat{\Psi}_d(z,t)$ and $\hat{\Psi}_b(z,t)$.

2.5.3 Dark-state polariton

As discovered by Fleischhauer and Lukin[86], we can equivalently introduce a new set of slow-light polaritonic excitations $\{\hat{\Psi}_d(z,t), \hat{\Psi}_b(z,t)\}$ as the normal modes of the system (Eqs. 2.75–2.76) in the weak signal approximation. Namely, we have

$$\hat{\Psi}_d(z,t) = \cos\theta_d(t)\hat{\mathcal{E}}_s(z,t) - \sin\theta_d(t)\hat{\mathcal{S}}(z,t) \tag{2.80}$$

$$\hat{\Psi}_b(z,t) = \sin\theta_d(t)\hat{\mathcal{E}}_s(z,t) + \cos\theta_d(t)\hat{\mathcal{S}}(z,t), \tag{2.81}$$

where $\hat{\mathcal{S}}(z,t) = \sqrt{N_A}e^{i(k_c^{\parallel}-k_s)z}\hat{\sigma}_{gs}(z,t)$ is the slowly-varying phase-matched collective spin operator, and $\theta_d = \arctan(g_d\sqrt{N_A}/\Omega_c)$ is the mixing angle. These operators are known as the dark-state (bright-state) polaritons $\hat{\Psi}_d(z,t)$ ($\hat{\Psi}_b(z,t)$), in direct analogy with the classic dark (bright) states $|d\rangle = \cos\theta_d|g\rangle - \sin\theta_d|s\rangle$ ($|b\rangle = \sin\theta_d|g\rangle + \cos\theta_d|s\rangle$) observed in coherent population trapping (chapter 6). These polaritons follow the quasi-bosonic commutation relations[86] (with the help of Eq. 2.25),

$$\left[\hat{\Psi}_{d,k}(t), \hat{\Psi}^{\dagger}_{d,k'}(t')\right] \simeq \left[\hat{\Psi}_{b,k}(t), \hat{\Psi}^{\dagger}_{b,k'}(t')\right] \simeq \delta_{kk'}\delta(t-t'), \tag{2.82}$$

where $\hat{\Psi}_d(z,t) = \frac{2\pi}{L}\int dk\hat{\Psi}_{d,k}(t)e^{ikz}$ and $\hat{\Psi}_b(z,t) = \frac{2\pi}{L}\int dk\hat{\Psi}_{b,k}(t)e^{ikz}$.

In the adiabatic limit, where $\Omega_c\hat{\sigma}_{gs} + g_d\hat{\mathcal{E}}_s e^{-i(k_c^{\parallel}-k_s)z} \simeq 0$ (Eq. 2.76), the bright-state polariton is $\hat{\Psi}_b \simeq 0$. In this limit, we can write the equation of motions for the dark-state polariton $\hat{\Psi}_d$ with the perturbation $\hat{\mathcal{S}}(z,t) \simeq -\frac{g_d\hat{\mathcal{E}}_s}{\Omega_c}$ (Eq. 2.77) as (ref.[86]),

$$\left(\frac{\partial}{\partial t} + v_g\frac{\partial}{\partial z}\right)\hat{\Psi}_d(z,t) = 0. \tag{2.83}$$

Thus, in the adiabatic regime, the dark-state polariton $\hat{\Psi}_d(z,t)$ follows the usual wave equation as in free-space with the group velocity $v_g = c\cos^2\theta_d$ determined by the 'amount' of the photonic component (signal field $\hat{\mathcal{E}}_s$; i.e., $\cos^2\theta_d$) in the polariton $\hat{\Psi}_d(z,t)$.

2.5.4 Adiabatic following of dark-state polariton

The dark state polariton $\hat{\Psi}_d(z,t) = \cos\theta_d(t)\hat{\mathcal{E}}_s(z,t) - \sin\theta_d(t)\hat{\mathcal{S}}(z,t)$ can be considered as a beamsplitter transformation between a signal mode $\hat{\mathcal{E}}_s(z,t)$ and a spin-wave mode $\hat{\mathcal{S}}(z,t)$, with the effective matter-light interaction Hamiltonian written as (Eq. 2.70)

$$\hat{H}^{(\text{map})}_{\text{int}} = i\dot{\theta}_d(z,t)\left(\hat{\mathcal{E}}_s(z,t)\hat{\mathcal{S}}^{\dagger}(z,t) - \hat{\mathcal{E}}^{\dagger}_s(z,t)\hat{\mathcal{S}}(z,t)\right). \tag{2.84}$$

We illustrate the adiabatic evolution of dark-state polariton $\hat{\Psi}_d$ in Fig. 2.5. At the initial step (1), with $\tau = 0$, we first apply a control laser with Rabi frequency $\Omega_c(z,t)$ (resonant to the $|e\rangle \rightarrow |s\rangle$) to open the

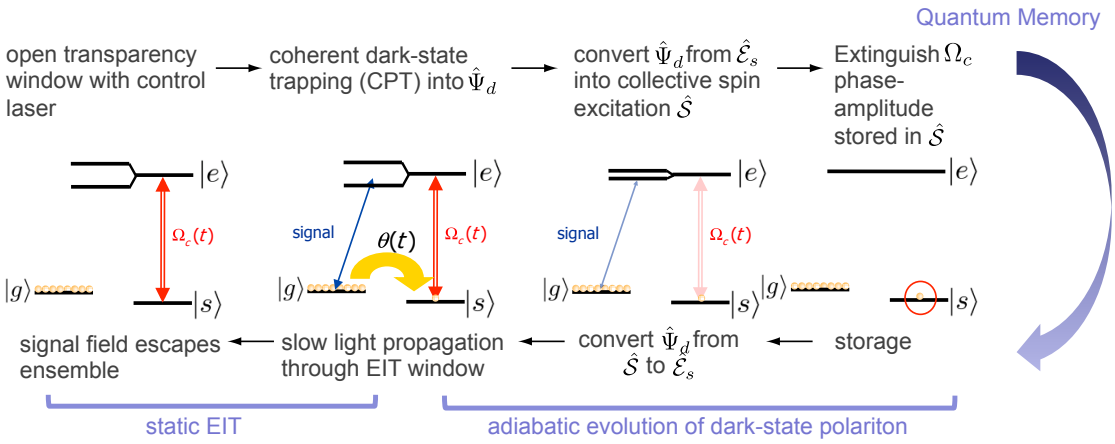

Figure 2.5: **Coherent evolution of dark state polariton.** First, we open the transparency window Ω_c with the control laser. As the signal field enters the EIT medium, it prepares the joint atom-field state in a dark state $\hat{\Psi}_d \simeq \hat{\mathcal{E}}_s(z,t)$. By adiabatically reducing the control laser's intensity to zero, we transfer the phase-amplitude information of the signal field $\hat{\mathcal{E}}_s(z,t)$ to the collective excitations $\hat{\mathcal{S}}(z,t)$. After a delay, we apply the control laser to coherently transfer the collective excitation $\hat{\mathcal{S}}(z,t)$ to the signal field $\hat{\mathcal{E}}_s(z,t)$ in a time reversal fashion. The signal field undergoes a slow-light propagation through the EIT medium, after which $\hat{\mathcal{E}}_s(z,t)$ escapes the ensemble.

transparency window in a counter-intuitive configuration[180] for the signal field $\hat{\mathcal{E}}_s(z,t)$, where the dark-state polariton $\hat{\Psi}_d = \hat{\mathcal{E}}_s$ is purely photonic (with $\Omega_c(z,t) \gg g_d\sqrt{N_A}$ and $\theta_d = 0$)[o]. In step (2), as the signal field enters the coherently dressed atomic media, the intensity for $\Omega_c(z,t)$ is adiabatically reduced to zero (thereby, $\theta_d = 0 \to \pi/2$), simultaneously decelerating the signal field[p] and transferring the phase-amplitude information of the photonic excitations $\hat{\mathcal{E}}_s$ to the collective atomic excitations $\hat{\mathcal{S}}$. In step (3), we store the spin-wave excitation for a controllable memory time τ. At the end of step (3), we apply the control laser in step (4) to reaccelerate the dark-state polariton $\hat{\Psi}_d$ back to the free-space velocity $v_g = c$, thereby coherently transferring the spin-wave amplitude $\hat{\mathcal{S}}$ back to the signal field $\hat{\mathcal{E}}_s$ (i.e., $\hat{\Psi}_d = \hat{\mathcal{S}} \to \hat{\mathcal{E}}_s$ with $\theta_d = \pi/2 \to 0$). Finally in step (5), the retrieved signal field $\hat{\mathcal{E}}_s$ propagates within the center of the transparency window with minimum absorption and escapes the EIT medium.

2.5.5 Non-adiabatic equations of motions

The dark-state polariton equation (Eq. 2.83) does not include any non-adiabatic terms, which account for the finite-bandwidth of the EIT medium and the non-adiabatic transitions between dark-state and bright-state polaritons[86,192]. More generally, we need to solve the complete equations of motions in Eqs. 2.71–2.74 with the weak signal approximation ($\sigma_{gg} \simeq 1 \gg \sigma_{ee}, \sigma_{ss}, \sigma_{es} \simeq 0$).

Here, we introduce a slowly-varying atomic polarization $\mathcal{P}(z,t) = \sqrt{N_A}\hat{\sigma}_{ge}$ induced by $\hat{\mathcal{E}}_s(z,t)$ in the

[o]For the single-excitation manifold, the dark state (Eq. 2.69) is $|\overline{g}_a, 1_s\rangle$, which is also the initial state of the system.

[p]The deceleration of the signal field is accompanied by a compression of the signal field due to the reduced group velocity v_g, where the tail of the wavepacket for the signal field catches up with the slowly propagating front part of the wavepacket. This allows us to 'fit' the signal field's wavepacket ($L_s \simeq 10$ m) within a small ensemble ($L \simeq 3$ mm).

dispersive coherent medium, and the slowly-varying phase-matched spin-wave operator $\hat{\mathcal{S}}(z,t) = \sqrt{N_A}\, e^{i(k_c^{\parallel}-k_s)z}\hat{\sigma}_{gs}$ defined in section 2.3.1.3. The dynamics of the signal field $\hat{\mathcal{E}}_s(z,t)$ and the spin-wave mode $\hat{\mathcal{S}}(z,t)$ is governed by a set of Heisenberg-Langevin equations (Eqs. 2.71–2.74),

$$(\partial_t + c\partial_z)\,\hat{\mathcal{E}}_s(z,t) = ig_d n_A(z)\frac{L}{\sqrt{N_A}}\hat{\mathcal{P}}(z,t) \tag{2.85}$$

$$\partial_t\hat{\mathcal{P}}(z,t) = -(\gamma_{ge}+i\Delta)\hat{\mathcal{P}}(z,t) + ig_d\sqrt{N_A}\hat{\mathcal{E}}_s(z,t) + i\Omega_c(z,t)\hat{\mathcal{S}} + \sqrt{2\gamma_{ge}}\hat{F}_P \tag{2.86}$$

$$\partial_t\hat{\mathcal{S}}(z,t) = -\gamma_{gs}\hat{\mathcal{S}}(z,t) + i\Omega_c^*(z,t)\hat{\mathcal{P}} + \sqrt{2\gamma_{gs}}\hat{F}_S. \tag{2.87}$$

Here, $\hat{F}_P$ and $\hat{F}_S$ are the respective δ-correlated Langevin noise operators for $\hat{\mathcal{P}}(z,t)$ and $\hat{\mathcal{S}}(z,t)$, with non-zero terms $\langle\hat{F}_P(z,t)\,\hat{F}_P^{\dagger}(z',t')\rangle = L\delta(z-z')\delta(t-t')$ and $\langle\hat{F}_S(z,t)\hat{F}_S^{\dagger}(z',t')\rangle = L\delta(z-z')\delta(t-t')$. Since the normally ordered noise operators $\langle\hat{F}_i^{\dagger}\hat{F}_i\rangle = 0$ with $i\in\{\mathcal{S},\mathcal{P}\}$ for vacuum reservoirs, we neglect them in the numerical calculation of chapter 6 (see section 2.3.1.2).

We emphasize that the collective enhancement ($\sqrt{N_A}$) of single atom-photon coupling constant g_d (Eqs. 2.85–2.87) enables a strong collective matter-light interaction with an effective coupling constant $g_{\text{eff}} = \sqrt{N_A}g_d$ between a single spin-wave of the ensemble and a single photon of the signal field. We are interested in the collectively enhanced storage (η_{s}) and retrieval (η_{r}) efficiency $\eta_{sr} = \eta_{\text{s}}\eta_{\text{r}}$ of the quantum field $\hat{\mathcal{E}}_s(z,t)$, which we define as the ratio of the number $\int dz\langle\hat{\mathcal{E}}_s^{\dagger}(z,t)\hat{\mathcal{E}}_s(z,t)\rangle$ of incoming photonic excitations in the signal field to the number of stored spin-wave excitations $\int dz\langle\hat{\mathcal{S}}^{\dagger}(z,t)\hat{\mathcal{S}}(z,t)\rangle$ (and vice versa). Specifically, for an atomic ensemble with finite optical depth $\tilde{d}_0$, there is an optimal control field $\Omega_c(z,t)$, which maximizes the transfer efficiency η_{sr}, by compromising two competing goals[186]: (1) The characteristic time variation δt_c in the control laser $\dot{\Omega}_c(z,t)$ must be slow relative to the two adiabatic criteria ($\Delta w_s \simeq \frac{2\pi}{\delta t_c} < \Delta w_{\text{EIT}}$ and $\delta t_c > \frac{\gamma_{eg}v_g}{g_d^2 N_A c}$), identified in section 2.5.2.2, to avoid dissipations of $\hat{\mathcal{P}}(z,t)$. A stronger control laser is preferable, as it provides a wider transparency window and minimizes spontaneous decay loss. On the other hand, (2) $\Omega_c(z,t)$ must small in order to localize and compress the incoming signal field's wavepacket ($L_s \simeq 10$ m) within the atomic sample ($L \simeq 3$ mm) to avoid significant leakage of the signal field.

2.5.5.1 Mapping photonic quantum states into and out of collective excitations

For a given optical depth $\tilde{d}_0$, there is an optimal Rabi frequency $\Omega_c(z,t)$ for the control field. In the experiment[30], we set $\tilde{d}_0$ and $\Omega_c(z,t)$ at 20 and 24 MHz, respectively. We show an example of our measurements of the EIT process for a single ensemble in Fig. 2.6, whereby we demonstrate the reversible mapping of a coherent state $|\alpha\rangle$ into and out the atomic memory ($|\alpha|^2 = 0.3$ per pulse). Because of finite $\tilde{d}_0$, the small length ($L = 3$ mm) of the ensemble and the turn-off time of $\Omega_c(z,t)$, we observe a considerable leakage in the storage process. The peak beyond $\tau \geq 1$ μs represents the retrieved pulse after $\tau \simeq 1$ μs of storage. Overall, we find an excellent agreement between our measurements and the numerical simulation following the coupled equations of motions in Eqs. 2.85–2.87. We use the fitted function of the input signal field as the initial state with all other parameters from independent measurements. We find an overall storage and

retrieval efficiency of $\eta_{sr} = 22 \pm 3\%$, similar to the theoretical prediction $\eta_{sr}^{\text{theory}} = 23\%$ (Fig. 2.6).

Experimentally, to avoid the dissipative absorption of the signal field $\hat{\mathcal{E}}_s(z,t)$ for our choice of polarization (σ_+ polarization), we optically pumped the atomic ensemble into a clock state $6S_{1/2}$, $|F = 4, m_F = 0\rangle$ with 90% efficiency. Initially, the strong control field $\Omega_c(z,t)$ (resonant with $6S_{1/2}, F = 3 \leftrightarrow 6P_{3/2}, F = 4$ transition with σ_+ polarization) opens the transparency window $\Omega_c(z,t) \simeq 24$ MHz for the signal mode. As the wave packet $\hat{\mathcal{E}}_s(z,t)$ of the signal field propagates through the ensemble, we extinguish the control fields $\Omega_c(z,t)$ in 20 ns, thereby coherently transforming the coherent state of the signal mode $\hat{\mathcal{E}}_{s,\text{in}}(z,t)$ to collective atomic excitation $\hat{\mathcal{S}}(z,t)$. After $\simeq 1.1$ μs, the atomic state is converted back to the signal mode $\hat{\mathcal{E}}_{s,\text{out}}(z,t)$ by switching on the control field $\Omega_c(z,t)$. We measure the normalized cross-correlation function for the input photonic state $\hat{\mathcal{E}}_{s,\text{in}}(z,t)$ with $g_{\text{in}}^{(2)} = 1.1 \pm 0.2$, as well as for the output photonic state $\hat{\mathcal{E}}_{s,\text{out}}(z,t)$ with $g_{\text{out}}^{(2)} = 1.0 \pm 0.2$, whereby we observe no degradation in the photon statistics.

In chapter 6, we discuss an experiment where we reversibly mapped a photonic entanglement into and out of quantum memories. We further examine the optimal control theory developed in ref.[188], where we theoretically apply the principle of time-reversal symmetry to optimize our reversible quantum interface.

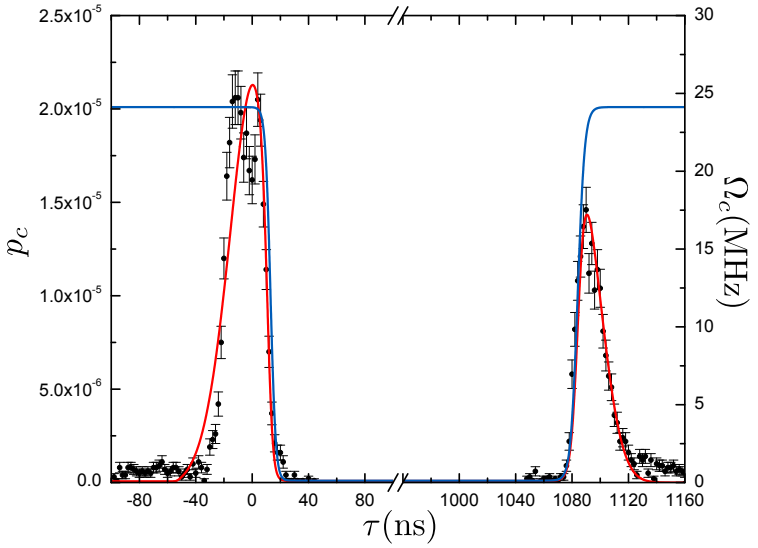

Figure 2.6: **Reversible mapping of a coherent state to and from an atomic memory.** The points around $\tau \simeq 0$ ns (i.e., -40 to 20 ns) represent the leakage of the signal field due to the finite optical depth and length of the ensemble. The points beyond $\tau \simeq 1$ μs show the retrieved signal field. The blue solid line is the estimated Rabi frequency $\Omega_c(z,t)$ of the control pulse, where we assumed $\Omega_c(t - z/c)$. The red solid curve is from a numerical calculation solving the equation of motion of the signal field in a coherently dressed medium (section 2.5.5). Error bars give the statistical error of 1 s.d for each point.

2.5.5.2 Collective enhancement: Reading spin waves

Heralded spin-waves generated from the parametric Raman interaction (section 2.3) can also be coherently transferred to photons in field 2 (with $\hat{\mathcal{E}}_s(z,t)$ replaced by $\hat{\mathcal{E}}_2(z,t)$). In particular, the initial states are $\hat{\mathcal{E}}_2(z,0) = 0$ and $\hat{\mathcal{S}}(z,0)$ with the spin-wave spatio-temporal mode $\hat{\mathcal{S}}(z,0)$ taken from the solution of Eqs. 2.47–2.48, evolved from the parametric interaction. We can then rigorously solve the non-adiabatic equations of motions (Eqs. 2.85–2.87) in the polaritonic picture. In practice, neglecting the spatio-temporal modes and self-consistent treatments of fluctuation and dissipation from first principles, we may model the mapping process as a beamsplitter transformation (a pseudo-model) from the spin-wave mode to the field 2 mode, where the readout noise is simulated by adding coherent-state reservoirs[193] (see chapter 9).

2.6 Decoherence

We have so far neglected the presence of spin-wave decoherence for $\hat{\sigma}_{gs}$ by setting $\gamma_{gs} = 0$ (e.g., neglecting spin-exchange collisions). Practically, this is a good approximation, given that the interaction times $\delta t_{w,r}$ for the writing and reading processes are fast compared to the relevant coherence times. However, if the delay τ between the storage and retrieval processes is longer than the coherence time τ_m of the spin waves, we must also include various spin-wave dynamics induced by the decoherence mechanisms. Here, we will review two major dissipative contributions[q] to spin-wave coherence in our experiment: (1) Inhomogeneous broadening and (2) motional dephasing.

2.6.1 Inhomogeneous broadening of spin waves

In our experiment, inhomogeneous broadenings of spin waves are dominated by two factors: (1) Inhomogeneous light shifts between $|g\rangle - |s\rangle$ (in the case of a nano-fiber trap in chapter 10), and from (2) inhomogeneous Zeeman broadening (see, e.g., chapters 4–5). Here, we describe a one-dimensional model[r] for the second type of decoherence mechanism. This model, however, should also be applicable to the first type of decoherence. The Zeeman decoherence model described in this section is similar to the one developed by Daniel Felinto [147].

We assume an initial atom-field state $\hat{\rho}_{\mathrm{a}\gamma_1} = \hat{\rho}_{\mathrm{a}}(0) \otimes \hat{\rho}_{\gamma_1}(0)$, where $\hat{\rho}_{\mathrm{a}}(0) = p_{m_{F_g}} |F_g, m_F\rangle\langle F_g, m_F|$ is the initial atomic state with Zeeman populations p_{m_F}, and $\hat{\rho}_{\gamma_1}(0) = |0_{\vec{k}_1}\rangle\langle 0_{\vec{k}_1}|$ is the initial vacuum state for field 1 (with all other modes traced over). In the single-excitation limit, a photoelectric event in field 1 (with unit detection efficiency) heralds an atomic state $\hat{\rho}_{\mathrm{a}}(t_w) = |\psi(t_w)\rangle_{\mathrm{a}}\langle\psi(t_w)|$ containing a single spin-wave excitation, with

$$|\psi(t_w)\rangle_{\mathrm{a}} = \frac{1}{\sqrt{N_A}} \left(\sum_i e^{i(\vec{k}_w \cdot \vec{r}_i - k_1 z_i)} |g_1, \cdots, g_{i-1}, \tilde{s}_i(t_w), g_{i+1}, \cdots, g_{N_A}\rangle \right), \tag{2.88}$$

where $e^{i(\vec{k}_w \cdot \vec{r}_i - k_1 z_i)}$ gives the phase-matching condition $(\vec{k}_w - \vec{k}_r) \cdot \vec{r}_i - (k_1 - k_2) z_i = 0$ during the reading process (section 2.6.2) and t_w is the time at the end of the write pulse. Here, given the initial atomic state $\hat{\rho}_{\mathrm{a}}(0)$ populated with multiple Zeeman sublevels, the single-atom spin flip $\tilde{s}_i(t_w)$ corresponds to a superposition of Zeeman-dependent hyperfine spin flips given by

$$|\tilde{s}_i(t_w)\rangle = \frac{1}{\sqrt{N_c}} \sum_{m_{F_g}, m_{F_s}} \sqrt{p_{m_{F_g}}} \sqrt{\xi^{q_w, q_1}_{m_{F_g}, m_{F_s}}} e^{i\mu_B \left(g_g m_{F_g} - g_s m_{F_s}\right) B_z(\vec{r}_i) t_w / \hbar} |s_{m_{F_s}}\rangle, \tag{2.89}$$

---

[q] Dispersive van der Waals interaction between the atomic dipoles $g_{vdW} \sim \frac{d_0^2}{4\pi\epsilon_0 r_{ij}^3}$ lead to a van der Waals dephasing for sufficiently high density. Generally, for high phase-space density, one may additionally consider elaborate collisional processes and radiation trapping [194] (due to imperfect optical pumping). Alternatively, the atoms can be trapped in an optical lattice to reduce collisional dephasing [116].

[r] The spatial variation of the magnetic field across the transverse directions can be neglected, given the aspect ratio of the atomic sample ($2w_0/L \simeq 2 \times 50\ \mu\mathrm{m}/3\ \mathrm{mm} \ll 1$). The inhomogeneous Zeeman broadening is thus dominated by the longitudinal inhomogeneity $B_z(z)$ of magnetic field.

where $N_c = \sum_{m_{F_g},m_{F_s}} \xi^{q_w,q_1}_{m_{F_g},m_{F_s}}$ is the normalization constant, $g_{g,s}$ are the respective g-factors for the ground states $\{|g\rangle,|s\rangle\}$, μ_B is the Bohr's magneton, $B_z(\vec{r}_i) = \vec{B}(\vec{r}_i)\cdot\hat{z}$ is the magnetic field projected along $\hat{z}$ at position $\vec{r}_i$, and $\xi^{q_w,q_1}_{m_{F_g},m_{F_s}}$ is the generalized effective coupling constant for the specific excitation pathway (see Eq. 2.49). Here, $q_{w,1}$ are the polarization helicities for the writing laser and the field 1.

This expression can be easily derived from $\xi = \tanh^2(i\int_0^\infty dt' \int_0^L dz \chi_p(z,t'))$ (Eq. 2.35) by generalizing the parametric coupling constant χ_p to accommodate Zeeman-dependent transition constants (which depends on the parameters $\{F_g, F_s, m_{F_g}, m_{F_s}, q_w, q_1\}$ via the various Cleabsh-Gordan coefficients). Alternatively, Eq. 2.89 can be derived from the mapping Hamiltonian $\hat{H}^{(\text{map})}_{\text{tot}}$. In writing Eqs. 2.88–2.89, I assumed the effective single-mode model for parametric interaction $\xi^{q_w,q_1}_{m_{F_g},m_{F_s}}$ in section 2.3.2.2, where the beam-waist of the writing laser is substantially larger than that of the quantum field. The Larmor precession of a single-atom spin-flip after a delay τ is then described by

$$\langle \tilde{s}_i(t_w+\tau)|\tilde{s}_i(t_w)\rangle = \frac{1}{N_c}\sum_{m_{F_g},m_{F_s}} p_{m_{F_g}} \xi^{q_w,q_1}_{m_{F_g},m_{F_s}} e^{i\mu_B\left(g_g m_{F_g} - g_s m_{F_s}\right)B_z(\vec{r}_i)\tau/\hbar}. \tag{2.90}$$

To understand the collective dynamics of $\hat{\rho}_{\text{a}}(\tau)$, we now calculate the overlap function ${}_{\text{a}}\langle\psi(t_w+\tau)|\psi(t_w)\rangle_{\text{a}}$ between the initial collective state and the final collective state, where the retrieval efficiency η_r is ideally proportional to $|{}_{\text{a}}\langle\psi(t_w+\tau)|\psi(t_w)\rangle_{\text{a}}|^2$ (section 2.5). If we assume that the atoms are stationary so that the phase-matching condition is preserved, using Eqs. 2.88–2.90, we obtain the following overlap,

$$\begin{aligned} {}_{\text{a}}\langle\psi(t_w+\tau)|\psi(t_w)\rangle_{\text{a}} &= \frac{1}{N_A N_c}\sum_{m_{F_g}} p_{m_{F_g}} \xi^{q_w,q_1}_{m_{F_g},m_{F_g}+q_w-q_1} \\ &\quad\times \int_0^L dz n(z) e^{i\mu_B\left((g_g-g_s)m_{F_g} - g_s(q_w-q_1)\right)B_z(z)\tau/\hbar}, \end{aligned} \tag{2.91}$$

where we made the continuum approximation for the summation $\sum_i \to \int dz n(z)$ and assumed pure polarization states ($q_{w,1}$) for the writing laser and the field 1 (i.e., $m_{F_s} = m_{F_g} + q_w - q_1$).

Assuming a flat-top atomic distribution $n(z) = N_A/L$ and a quadratically inhomogeneous Zeeman shift $B_z(z) = (4\delta B_z/L^2)(z-L/2)^2$, we obtain

$${}_{\text{a}}\langle\psi(t_w+\tau)|\psi(t_w)\rangle_{\text{a}} = \frac{1}{N_c\sqrt{L}}\sum_{m_{F_g}} p_{m_{F_g}} \xi^{q_w,q_1}_{m_{F_g},m_{F_g}+q_w-q_1} f_d(\tau), \tag{2.92}$$

where the decay amplitude $f_d(\tau)$ for the Raman transition $m_{F_g} \to m_{F_s} = m_{F_g} + q_w - q_1$ is given by

$$f_d(\tau) = -\frac{\sqrt{i\pi}\,\text{erf}\left(\sqrt{-i\alpha_{m_{F_g}}\tau}\right)}{2\sqrt{\alpha_{m_{F_g}}\tau}}, \tag{2.93}$$

with a Zeeman-dependent decay constant $\alpha_{m_{F_g}} = \mu_B((g_g-g_s)m_{F_g} - g_s(q_w-q_1))\delta B_z/\hbar$. The function $\text{erf}(x) = \frac{2}{\sqrt{\pi}}\int_0^x dx' e^{-x'^2}$ is the error function. In Fig. 2.7, we show the result of our calculation

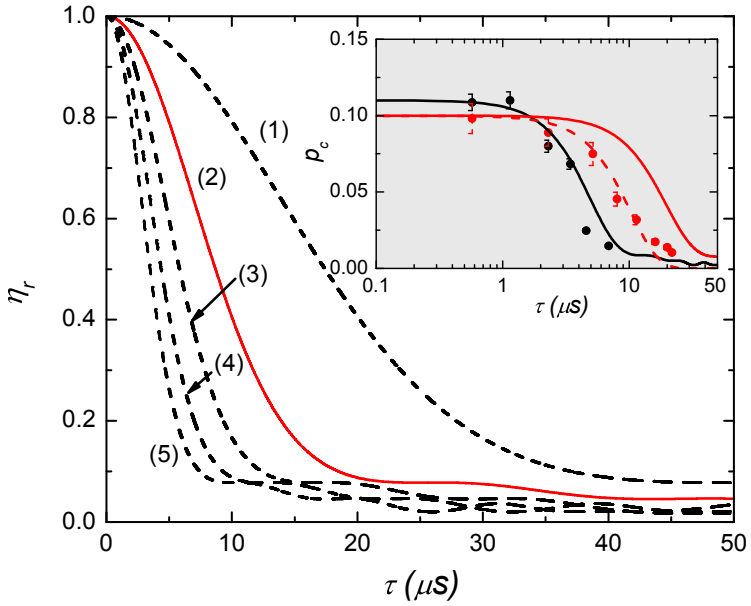

Figure 2.7: **Spin-wave decoherence due to inhomogeneous Zeeman broadening.** We show the normalized retrieval efficiency based on the theoretical expression $\eta_r \sim |_{\rm a}\langle\psi(t_w+\tau)|\psi(t_w)\rangle_{\rm a}|^2$ (Eq. 2.93) as a function of storage time τ, for (1) $\delta B_z = 10$, (2) 20, (3) 30, (4) 40, and (5) 50 mG. A typical experimental value for the inhomogeneous Zeeman broadening is $\delta B_z = 20$ mG (red line), after nulling the magnetic fields with bias coils (based on our measurement of off-resonant Raman spectroscopy [195]). We assumed the length of the ensemble to be $L = 3$ mm. The atomic cloud is initially prepared in the ground state $|g\rangle$ with uniform Zeeman distribution $p_{m_{F_g}} = 1/F_g$. In this calculation, $\{|g\rangle, |s\rangle, |e\rangle\}$ denote the levels $\{|6S_{1/2}, F = 4\rangle, |6S_{1/2}, F = 3\rangle, |6P_{3/2}, F = 4\rangle\}$. (inset) We measure the conditional probability p_c to detect a single-photon in field 2 as a function of τ. The expected Zeeman dephasing is $\tau_d \simeq 30$ μs (red line) at $\delta B_z \simeq 10$ mG (based on Raman spectroscopy), whereas the measured coherence time is only $\tau_d \simeq 12$ μs (red points). This result is consistent with the theoretical prediction for motional dephasing (red dashed line) in Fig. 2.8. For reference, we also plot the spin-wave coherence measurements at $\delta B_z \simeq 30$ mG (black points), which are consistent with Zeeman dephasing (black line). The vertical axes of the theory (black, red) lines for η_r are scaled to fit the experimental data for the photoelectric detection probability p_c of the field 2.

of the retrieval efficiency η_r after storage time τ. Note that the second-order approximation $B_z(z) = (4\delta B_z/L^2)(z - L/2)^2$ is reasonable for our experiment, since the Helmholtz bias coils can in principle cancel inhomogeneous Zeeman broadening only up to the first-order. Collective Larmor rephasing (oscillation in η_r at long τ), also known as dark-state polariton collapse and revival [119,120], is suppressed in our case of inhomogeneous Zeeman broadening by the additional factor of $2\sqrt{\alpha_{m_{F_g}}\tau}$ in the denominator.

Generally, the temporal profile of the spin-wave dephasing $\eta_r(\tau)$ due to Zeeman broadening depends on both the number density $n(z)$ and the inhomogeneous magnetic field $B_z(z)$ across the sample. Practically, the atomic density is approximately a Gaussian distribution $n(z) \sim e^{-4z^2/L^2}$ in our experiment. If we assume that the first-order (linear) Zeeman shift is dominant, with $B_z(z) = (\delta B_z/L)z$, the equivalent expression for $\langle\tilde{s}(t_w+\tau)|\tilde{s}(t_w)\rangle$ (see, e.g., Eq. 2.91) simply depicts a Fourier transform of $n(z)$, which results in a Gaussian decay of η_r. Thus, the temporal profile of $\eta_r(\tau)$ may provide some information about the spatial inhomogeneity of the Zeeman levels, given the measured atomic density $n(z)$.

2.6.2 Motional dephasing of spin waves

As seen in Eq. 2.88, the spin-wave dynamics is also dictated by the spatial coherence $\vec{k}_w \cdot \vec{r}_i - k_1 z_1$ of the spin-wave, which preserves the phase-matching condition required for collective enhancement. Here, we provide a simple model for motional dephasing

We first assume a linear atomic motion by $\vec{r}_i(t_w + \tau) = \vec{r}_i(t_w) + \vec{v}_i \tau$ during the storage time τ for the i^{th} atom. The final collective state after motional dephasing can thus be written as

$$|\psi(t_w + \tau)\rangle_{\text{a}} = \frac{1}{\sqrt{N_A}} \left(\sum_i e^{i\delta k (y_i(t_w) + v_{y,i}\tau)} |g_1, \cdots, g_{i-1}, \tilde{s}_i, g_{i+1}, \cdots, g_{N_A}\rangle \right), \tag{2.94}$$

where $\delta k = |\vec{k}_w - \vec{k}_1| \simeq k_w \sin\theta_{w1}$ is the net momentum transfer to the spin-wave (with a small angle approximation $\theta_{w1} \ll 1$ between the k-vectors of the writing laser and field 1 on the $y - z$ plane) and $v_{y,i} = \vec{v}_i \cdot \hat{y}$ is the atomic velocity projected along $\hat{y}$.

As we discussed in section 2.6.1, the retrieval efficiency is proportional to the overlap $|_{\text{a}}\langle\psi(t_w+\tau)|\psi(t_w)\rangle_{\text{a}}|^2$. If we assume a continuum limit for the momentum distribution $g(v)$ of the thermal atoms, the overlap is given by

$$_{\text{a}}\langle\psi(t_w + \tau)|\psi(t_w)\rangle_{\text{a}} \quad = \quad \int dv g(v) e^{i\delta k v \tau}. \tag{2.95}$$

For thermal atoms at T_d, as in our case of laser-cooled Cesium atoms $T_d \simeq 100\ \mu$K, the atomic motion follows the Maxwell-Boltzmann distribution $g(v) = e^{-mv^2/2k_B T_d}$. The retrieval efficiency $\eta_r(\tau) \sim |_{\text{a}}\langle\psi(t_w + \tau)|\psi(t_w)\rangle_{\text{a}}|^2$ is then (Fourier-transforming $g(v)$)

$$\eta_r = e^{-\tau^2/\tau_d^2}, \tag{2.96}$$

where $\tau_d = \lambda_s/2\pi v_s$ with $v_s = \sqrt{2k_B T_d/m}$. Here, we defined the spatial coherence length $\lambda_s = 2\pi/\delta k$ for the spin-wave with momentum transfer δk.

In Fig. 2.8, we show the temporal profile of the normalized retrieval efficiency η_r as a function of storage time τ (Eq. 2.96) for various temperatures T_d and for two different angles $\theta_{w1} \simeq 3^\circ$ ($\theta_{cs} \simeq 2^\circ$) between the two fields (thereby, varying the coherence length λ_s of the spin-wave). I note that there are two relevant factors which fully characterize the motional dephasing τ_d: (1) Atomic motion v_s and (2) spin-wave coherence length λ_s. By decreasing the temperature T_d of the atomic sample, we can reduce the mean velocity $v_s = \sqrt{2k_B T_d/m}$, and thereby increase the coherence time, as shown in Fig. 2.8. By placing an optical lattice along the momentum transfer $\delta\vec{k} \parallel \hat{y}$[s], the atomic motion can also be dramatically reduced[115–117,196] (see also Fig. 1.3 in chapter 1). On the other hand, to improve τ_c, it is also possible to increase the spin-wave coherence length $\lambda_s = 2\pi/\delta k$ for a given v_s (Fig. 2.8) by moving to a collinear geometry ($\vec{k}_w \parallel \vec{k}_1$) with

[s] In this case, it is important to also consider the inhomogeneous light shifts between $|g\rangle - |s\rangle$ from the optical lattice, as discussed in the previous section.

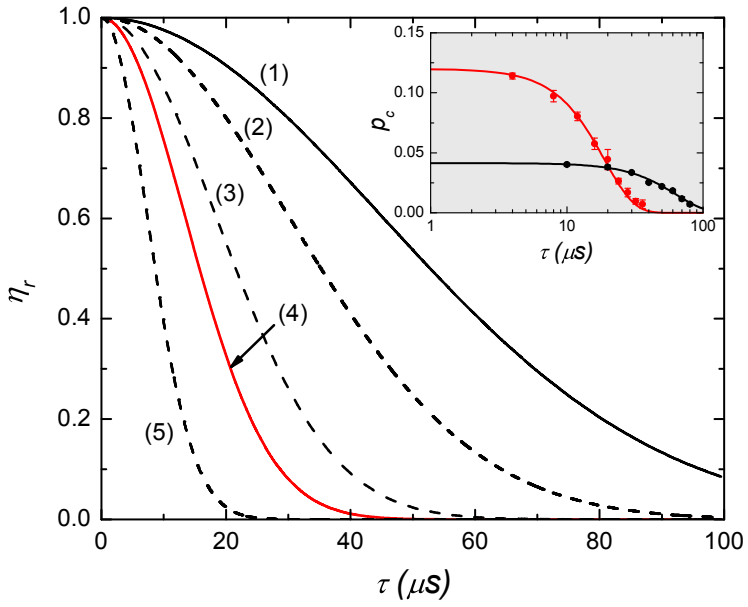

Figure 2.8: **Spin-wave dephasing due to atomic motion.** We show the normalized retrieval efficiency based on the theoretical expression $\eta_r \sim |_{\rm a}\langle\psi(t_w+\tau)|\psi(t_w)\rangle_{\rm a}|^2$ (Eq. 2.96) as a function of storage time τ, for (1) $T_d = 30$ μK (with $\theta_{w1} = 2°$), and for (2) $T_d = 80$ μK (with $\theta_{w1} = 3°$), (3) $T_d = 150$ μK (with $\theta_{w1} = 3°$), (4) $T_d = 250$ μK (with $\theta_{w1} = 3°$), (5) $T_d = 550$ μK (with $\theta_{w1} = 3°$). (inset) A typical experimental value for the motional dephasing is $\tau_d \simeq 20$ μs ($T_d \simeq 150$ μK, $\theta_{w1} \simeq 3°$), as shown in the inset with experimental data (red points) and theory line (3) (red line). After optimizing polarization gradient cooling ($T_d \simeq 30$ μK) and optical pumping to clock state $|F = 4, m_F = 0\rangle$ (along with the increase in the spin-wave coherence length via $\theta_{cs} \simeq 2°$), we further achieve a memory time of ~ 65 μs (black points) for storing and retrieving a coherent state. The vertical axes of the theory (black, red) lines for η_r are scaled to fit the experimental data for the photoelectric detection probability p_c of the fields (signal field, field 2).

Zeeman storage (at the magic magnetic field), thereby to $\delta\vec{k} = \vec{k}_w - \vec{k}_1 \simeq 0$ (with coherence length $\lambda_s \simeq 3$ cm $\gg L, w_0$ eventually extending beyond the size of the atomic sample). In this case, the storage time τ due to atomic motion will be limited by the collisional dephasing[116,117] and by the loss of atoms from the excitation volume[78].

In the inset of Fig. 2.8, we show our measurement for the decay of the (conditional) photoelectric detection probability p_c of a signal (field 2) pulse after a storage time τ for a coherent state $|\alpha\rangle$ with $|\alpha|^2 \simeq 0.9$ per pulse (for a heralded collective excitation), shown by black (red) points. In particular, after cooling the atoms to $T_d \simeq 30$ μK, optical pumping to the clock state, and increasing the spin-wave coherence length by reducing $\theta_{cs} = 3° \to 2°$, we achieve a memory time of ~ 65 μs for storing and retrieving a coherent state, a substantial improvement relative to the result in chapter 6.